

AD-A167 204

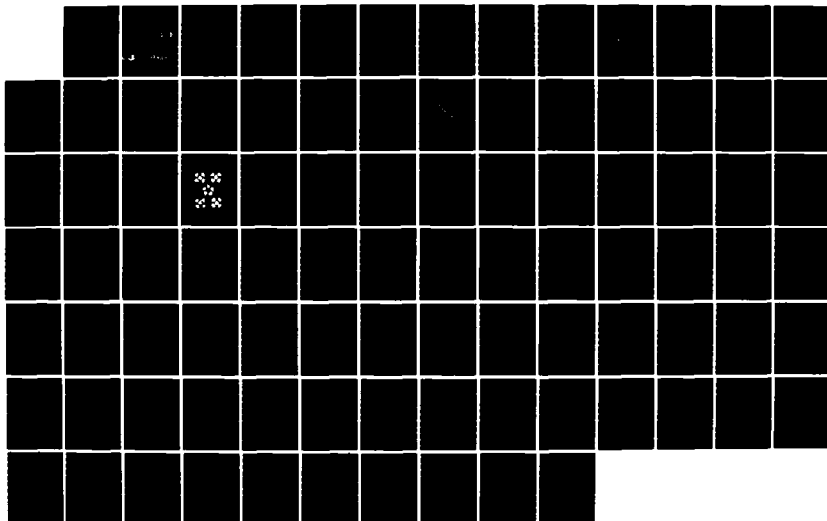
THE DEVELOPMENT OF MICRO-CONCRETE FOR SCALE MODEL
TESTING OF BURIED STRUC. (U) FLORIDA UNIV GAINESVILLE
DEPT OF CIVIL ENGINEERING C H CUNNINGHAM ET AL. JAN 86
ESL-TR-85-49 F00635-83-C-0136

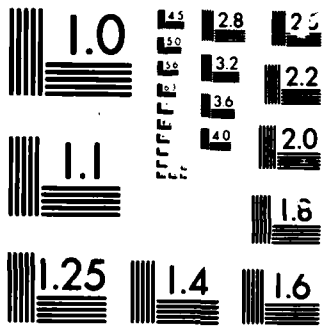
1/1

UNCLASSIFIED

F/G 11/2

NL





MICROCOPY

CHART

AD-A167 284

ESL-TR-85-49

2

The Development of Micro-Concrete for Scale Model Testing of Buried Structures

C. H. CUNNINGHAM
F. C. TOWNSEND
F. E. FAGUNDO

UNIVERSITY OF FLORIDA
DEPARTMENT OF CIVIL ENGINEERING
GAINESVILLE, FL 32611

FINAL REPORT

JANUARY 1986

SEPTEMBER 1983 - DECEMBER 1984

DTIC
ELECTE
MAY 09 1986
S D

APPROVED FOR PUBLIC RELEASE: DISTRIBUTION UNLIMITED



AFESC

ENGINEERING & SERVICES LABORATORY
AIR FORCE ENGINEERING & SERVICES CENTER
TYNDALL AIR FORCE BASE, FLORIDA 32403

86 5 8 024

NOTICE

PLEASE DO NOT REQUEST COPIES OF THIS REPORT FROM
HQ AFESC/RD (ENGINEERING AND SERVICES LABORATORY).
ADDITIONAL COPIES MAY BE PURCHASED FROM:

NATIONAL TECHNICAL INFORMATION SERVICE
5285 PORT ROYAL ROAD
SPRINGFIELD, VIRGINIA 22161

FEDERAL GOVERNMENT AGENCIES AND THEIR CONTRACTORS
REGISTERED WITH DEFENSE TECHNICAL INFORMATION CENTER
SHOULD DIRECT REQUESTS FOR COPIES OF THIS REPORT TO:

DEFENSE TECHNICAL INFORMATION CENTER
CAMERON STATION
ALEXANDRIA, VIRGINIA 22314

UNCLASSIFIED

ADA 167284

SECURITY CLASSIFICATION OF THIS PAGE

REPORT DOCUMENTATION PAGE

1a. REPORT SECURITY CLASSIFICATION Unclassified			1b. RESTRICTIVE MARKINGS										
2a. SECURITY CLASSIFICATION AUTHORITY			3. DISTRIBUTION/AVAILABILITY OF REPORT Approved for public release. Distribution Unlimited.										
2b. DECLASSIFICATION/DOWNGRADING SCHEDULE			5. MONITORING ORGANIZATION REPORT NUMBER(S) ESL-TR-85-49										
4. PERFORMING ORGANIZATION REPORT NUMBER(S)			7a. NAME OF MONITORING ORGANIZATION Air Force Engineering and Services Center										
6a. NAME OF PERFORMING ORGANIZATION University of Florida		6b. OFFICE SYMBOL (if applicable)	7b. ADDRESS (City, State and ZIP Code) HQ AFESC/RDCS Tyndall AFB FL 32403-6001										
6c. ADDRESS (City, State and ZIP Code) University of Florida Department of Civil Engineering Gainesville, FL 32611			9. PROCUREMENT INSTRUMENT IDENTIFICATION NUMBER Contract # F08635-83-C-0136 Task No. 83-1										
8a. NAME OF FUNDING/SPONSORING ORGANIZATION Air Force Eng. & Services Center		8b. OFFICE SYMBOL (if applicable) RDCS	10. SOURCE OF FUNDING NOS.										
8c. ADDRESS (City, State and ZIP Code) HQ AFESC/RDCS Tyndall AFB, FL 32403-6001		<table border="1"> <tr> <th>PROGRAM ELEMENT NO.</th> <th>PROJECT NO.</th> <th>TASK NO.</th> <th>WORK UNIT NO.</th> </tr> <tr> <td>62206F</td> <td>2673</td> <td>0048</td> <td></td> </tr> </table>				PROGRAM ELEMENT NO.	PROJECT NO.	TASK NO.	WORK UNIT NO.	62206F	2673	0048	
PROGRAM ELEMENT NO.	PROJECT NO.	TASK NO.	WORK UNIT NO.										
62206F	2673	0048											
11. TITLE (Include Security Classification) The Development of Micro-Concrete for Scale Model Testing of Buried Structures													
12. PERSONAL AUTHOR(S) C. H. Cunningham, F. C. Townsend, F.E. Fagundo													
13a. TYPE OF REPORT Final		13b. TIME COVERED FROM 09/83 TO 12/84		14. DATE OF REPORT (Yr., Mo., Day) January 1986									
15. PAGE COUNT 84													
16. SUPPLEMENTARY NOTATION Availability of this report is specified on reverse of front cover.													
17. COSATI CODES			18. SUBJECT TERMS (Continue on reverse if necessary and identify by block number)										
FIELD	GROUP	SUB. GR.	Reinforced Concrete Microconcrete										
13	13		Centrifugal Models Blast Loading										
11	04												
19. ABSTRACT (Continue on reverse if necessary and identify by block number)													
<p>This report describes the development of microconcrete and miniaturized reinforcement for modelling 1/50th and 1/90th scale reinforced concrete buried structures. The microconcrete uses gypsum cement, sand aggregate and water in a ratio of 1:0.8:0.25 by weight. Curing is halted by sealing the microconcrete after 48 hours exposure to air at ambient temperatures. The resulting mix has the following properties:</p> <p>$f'_c = 4085 \text{ psi}$, $f'_t = 327 \text{ psi}$, $\gamma = 130 \text{ pcf yd}$, $E_c = 3.3 \times 10^6 \text{ psi}$.</p> <p>Miniaturized reinforcement was developed using 2R, 24, and 22-gage wire passed through a deforming machine to provide knurls on the wire. Pretensioning the wire was necessary to remove kinks and coils. Failure load predictions of miniature reinforced beams agreed well with observed results.</p>													
20. DISTRIBUTION/AVAILABILITY OF ABSTRACT UNCLASSIFIED/UNLIMITED <input checked="" type="checkbox"/> SAME AS RPT <input type="checkbox"/> DTIC USERS <input type="checkbox"/>			21. ABSTRACT SECURITY CLASSIFICATION Unclassified										
22a. NAME OF RESPONSIBLE INDIVIDUAL JOHN R. HAYES, JR		22b. TELEPHONE NUMBER (Include Area Code) 904-283-6365		22c. OFFICE SYMBOL RDCS									

DD FORM 1473, 83 APR

EDITION OF 1 JAN 73 IS OBSOLETE.

Unclassified

SECURITY CLASSIFICATION OF THIS PAGE

PREFACE

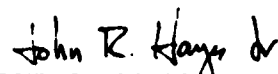
This report was prepared by the Department of Civil Engineering, University of Florida, Gainesville, Florida, 32611, under Contract Number F08635-83-C-0136, Task No. 83-1, for the Air Force Engineering and Services Center, Engineering and Services Laboratory, Engineering Research Division, Tyndall Air Force Base, Florida, 32403-6001, under Job Order Number 26730022.

This report is published as submitted to the University of Florida by Mr Charles H. Cunningham, as his Master of Engineering report under the direction of Professors F. C. Townsend, M. C. McVay and F. E. Fagundo. Captain Paul L. Rosengren, Jr, was the HQ AFESC/RDCS Project Officer. This report summarizes work performed between September 1983 and December 1984.

This report presents the development of a microconcrete mix using gypsum cement and miniaturized reinforcement using deformed 28, 24 and 22 gage wire for casting 1/60 and 1/90 scale buried structures.

This report has been reviewed by the Public Affairs Office (PA) and is releasable to the National Technical Information Service (NTIS). At NTIS, it will be available to the general public, including foreign nationals.

This technical report has been reviewed and is approved for publication.


JOHN R. HAYES, JR
Project Officer


ROBERT E. BOYER, Colonel, USAF
Director, Engineering and Research
Laboratory

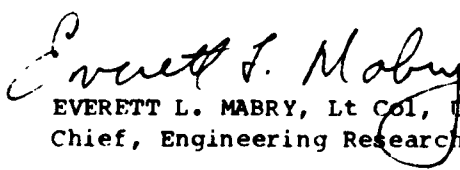

EVERETT L. MABRY, Lt Col, USAF
Chief, Engineering Research Division

TABLE OF CONTENTS

	Page
LIST OF FIGURES.....	v
LIST OF TABLES.....	vii
SECTION I INTRODUCTION.....	1
SECTION II MODELLING THEORY.....	4
SECTION III LITERATURE REVIEW.....	8
A. MODEL CONCRETE.....	8
B. MODEL REINFORCEMENT.....	17
SECTION IV DEVELOPMENT OF MICROCONCRETE MIX.....	21
SECTION V DEVELOPMENT OF MINIATURIZED REINFORCEMENT.....	35
SECTION VI MICROCONCRETE MINIATURIZED REINFORCEMENT INTERACTION....	45
SECTION VII DEVELOPMENT OF STRUCTURAL MODELS.....	54
A. BACKGROUND.....	54
B. SINGLE BAY WITH BURSTER SLAB - 1/90 SCALE MODEL.....	54
C. DOUBLE BAY WITH BURSTER SLAB - 1/90 SCALE MODEL.....	55
D. SINGLE BAY WITH BURSTER SLAB - 1/60 SCALE MODEL.....	55
E. GENERAL.....	55
SECTION VIII CONCLUSION AND RECOMMENDATION.....	73
REFERENCES	75
APPENDIX A MODELLING MATERIALS AND PROCEDURES.....	77



Accession For	
NTIS CRA&I	<input checked="" type="checkbox"/>
DTIC TAB	<input type="checkbox"/>
Unannounced	<input type="checkbox"/>
Justification	
By	
Distribution /	
Availability Codes	
Dist	Avail and/or Special
A-1	

LIST OF FIGURES

FIGURE	TITLE	PAGE
1	PROTOTYPE STRUCTURE.....	2
2	EXAMPLES OF STRESS VS STRAIN PLOTS RESULTING IN DISTORTED MODELS.....	7
3	APPROXIMATE RETARDING EFFECT OF USG SODATE RETARDER ON MOLDING, CASTING OR POTTERY PLASTERS.....	13
4	EFFECT OF WATER-GYPSUM RATIO ON f'_c	15
5	EFFECT OF AGGREGATE CONCENTRATION ON f'_c	15
6	STRENGTH-AGE RELATIONS FOR GYPSUM MORTARS.....	16
7	EFFECT OF DEFORMATION AND HEAT TREATMENT ON STRESS-STRAIN BEHAVIOR OF REINFORCING WIRE.....	20
8	CHART TO SHOW AGGREGATE ROUNDNESS CLASSES.....	23
9	AGGREGATE GRADATION CURVES FOR PROTOTYPE AND MODEL.....	26
10	COMPRESSION LOAD VERSUS STRAIN FOR MICROCONCRETE.....	29
11	SCHEMATIC: TENSILE TEST OF REINFORCEMENT MATERIAL.....	40
12	DETAIL CONNECTION.....	40
13	STRESS-STRAIN RELATION FOR TENSILE TESTING OF MODEL REINFORCEMENT.....	42
14	SCHEMATIC OF BEAM, AND LOCATION OF LOADING AND SUPPORTS USED IN BEAM TESTS.....	46
15	REINFORCED BEAM TESTS AND NONSAP PREDICTION.....	48
16	NONSAPC MODEL.....	50
17	PROTOTYPE STRUCTURAL DETAILS.....	57
18	STRUCTURAL DETAILS - 1/90 SCALE SINGLE BAY MODEL.....	60
19	STRUCTURAL DETAILS - 1/90 SCALE DOUBLE BAY MODEL.....	64
20	STRUCTURAL DETAILS - 1/60 SCALE SINGLE BAY MODEL.....	68
21	STRUCTURAL DETAILS - MODEL BURSTER SLABS.....	72

LIST OF TABLES

TABLE	TITLE	PAGE
1	SIMILITUDE REQUIREMENT OF REINFORCED CONCRETE MODELS UNDER STATIC LOAD.....	6
2	RESULTS OF COMPRESSION TESTS FOR VARIOUS TRIAL MIXES.....	24
3	RESULTS OF MICROCONCRETE TENSILE TESTS FOR MIX 1 ⁵ -.8-.25.....	31
4	RESULTS OF MICROCONCRETE RUPTURE MODULUS TESTS FOR.....	32
5	RESULTS OF ADDITIONAL COMPRESSION TESTS PERFORMED ON MIX 1 ⁵ -.8-.25.....	34
6	DEFORMED BAR DESIGNATION NUMBERS, NOMINAL WEIGHTS, NOMINAL DIMENSIONS AND DEFORMATION REQUIREMENTS.....	37
7	STANDARD UNITED STATES REINFORCING BARS; FULL SCALE, 1/60 SCALE AND 1/90 SCALE.....	38
8	MINIATURIZED REINFORCEMENT: WEIGHTS, DIMENSIONS, AND DEFORMATION SPECIFICATIONS.....	44
9	SUMMARY OF STEEL REINFORCEMENT QUANTITIES.....	59

SECTION I

INTRODUCTION

The design of a structure is based on its anticipated response to loading since direct full-scale testing is usually impractical due to the magnitude of most structures and the actual imposed loads. However, physical modelling applies when (a) no suitable analytical methods exist for estimating structural response, (b) a physical test is necessary to corroborate behavior that is predicted by analytical methods or, (c) when model testing may be competitive in cost with analytical methods.

The Department of Defense is responsible for many protective structures which may be subjected to explosive loadings. The large degree of uncertainty associated with explosive loadings makes the application of simple design safety factors insufficient and thus, this premises the need for intensive and comprehensive testing programs to assure reliable structural performance for an anticipated threat.

In the past, the Department of Defense engaged itself in full-scale testing of structures at tremendous costs and safety risks. Scaled models ranging from one-half to one-twentieth of the size of the prototype have also been used but again suffer from cost and safety restrictions. Additionally, there are concerns that testing smaller than one-tenth the prototype size at normal gravity is limited because the dead load created by the structure itself greatly affects dynamic response (Reference 1).

As a possible solution to these problems, the Air Force has initiated investigations concerning the feasibility of centrifugally modelling protective structures subjected to blast loadings at a substantially reduced scale. The prototype structure, which is buried some 6 feet below ground surface, is presented in Figure 1. A burster slab provides protection from direct explosive loading. With present centrifuges, the prototype shelter could be tested in its entirety at 1/150 to 1/300 scale, or components could be tested at a larger scale.

However, the major concerns in this approach are (a) the ability to construct such a small model and (b) the ability to model materials (reinforced concrete, specifically) at these scales. The scaling laws that ensure similitude between model and prototype have been investigated and reported by Bradley, Townsend, Fagundo, and Davidson (Reference 2). This report investigates development of the materials needed to construct the model to satisfy the similitude requirements, combined with the feasibility of modelling at these greatly reduced scales.

SECTION II

MODELLING THEORY

The governing relationship between a full-scale prototype and small-scale model are based on the theory of similitude and Buckingham's π Theorem. These theories are developed in most textbooks dealing with modelling techniques. A good introduction is presented in Reference 1.

The scale factor S_i is the multiplier required to convert any model quantity, i_m , to its corresponding prototype quantity, i_p ; or

$$i_p = S_i i_m \rightarrow S_i = \frac{i_p}{i_m}$$

In a static problem, only two fundamental dimensions are involved: force and length. Therefore, in order to have a true model, only two independent scale factors are allowed; usually S_σ and S_L . Other scale factors are then formulated based on the two independent factors.

If, however, one additional independent scale factor is introduced, such as S_ϵ for strain, the model becomes distorted. This is the case when the stress-strain curves of one or more of the modelling materials differs from its corresponding prototype material, or $S_\epsilon \neq 1$. One of many cases of $S_\epsilon \neq 1$ for reinforced concrete is shown in Figure 2 where the stress-strain curves of the prototype and the model differ for both the reinforcement and concrete. While the use of an independent strain scale provides more freedom in the modelling process, it complicates the

analysis, and the complications are increased when the effects of large deformations are to be considered during testing.

Table 1 is a summary of scale factors for reinforced concrete models. It is based on the tables presented in the American Concrete Institute (ACI) and the American Society of Agricultural Engineers modelling publications (References 3 and 4).

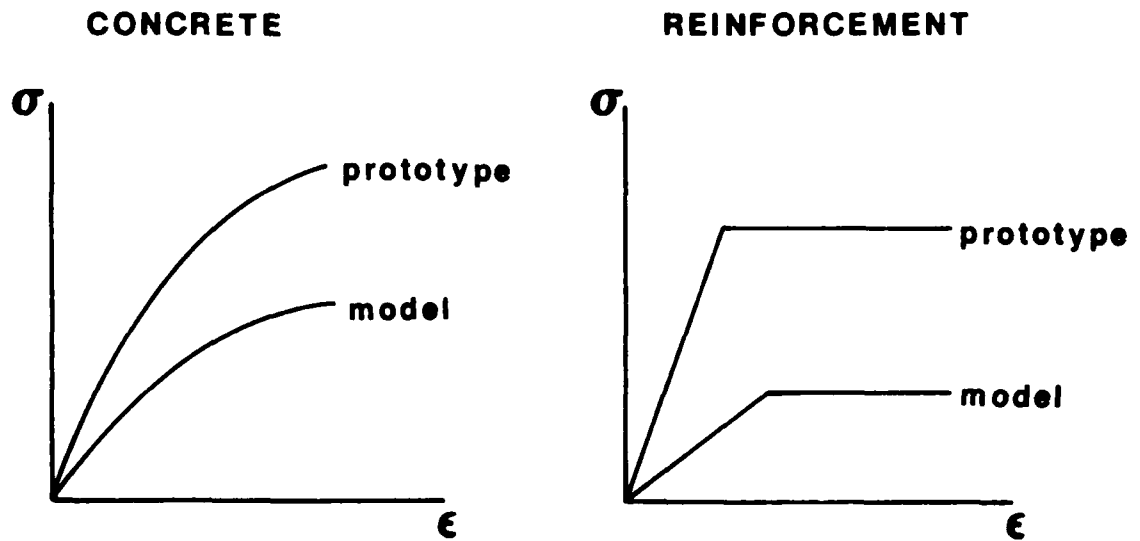
Column 4 shows how the two independent scale factors, S_o and S_x are applied to a true reinforced concrete model. Column 5, based on the reinforcement plot in Figure 2, shows the effects caused by introducing the additional independent strain scale factor, $S_e \neq 1$. The addition of the factor, S_e , into the displacement equation, $\delta_p = S_e S_x \delta_m$, shows how complicated the modelling analysis can become when deformations are to be considered, especially with the anisotropic conditions of a two-material system such as reinforced concrete.

In scaling models for centrifuge testing, $S_x = S_n$ (Reference 2), where n equals the number of gravities at which the model is to be tested. In other words, a reduction in the linear dimension of the prototype from one to 60 corresponds to 60 g centrifugal testing. The basis of the scales used in this research is the desired centrifugal acceleration.

The effort of this research is directed toward the development of a true model. A table similar to Table 1 appears in Section VIII and shows the final scale factors for the materials developed.

TABLE 1. Similitude Requirement of Reinforced
Concrete Models Under Static Load
(from References 3 and 4)

(1) Quantity	(2) Dimension	(3) Prototype Dimension	True Model (4) Scale: Length stress	Distorted Model Scale: length stress, strain, Modulus $E_p/E_m \neq S_\sigma/S_\epsilon$ (5)
Linear Dimension	L	ℓ_p	$\ell_p = S_\ell \ell_m$	$\ell_p = S_\ell \ell_m$
Area of Reinforcement	L^2	A_{rp}	$A_{rp} = S_\ell^2 A_{rm}$	$A_{rp} = S_\sigma S_\ell^2 E_{rm} S_\epsilon^{-1} E_p A_{rm}$
Displacement	L	δ_p	$\delta_p = S_\ell \delta_m$	$\delta_p = S_\epsilon S_\ell \delta_m$
Concrete Stress	FL^{-2}	σ_{cp}	$\sigma_{cp} = S_\sigma \sigma_{cm}$	$\sigma_{cp} = S_\sigma \sigma_{cm}$
Concrete Modulus	FL^{-2}	E_{cp}	$E_{cp} = S_\sigma E_{cm}$	$E_{cp} = S_\sigma S_\epsilon^{-1} E_{cm}$
Reinforcement Stress	FL^{-2}	σ_{rp}	$\sigma_{rp} = S_\sigma \sigma_{rm}$	$\sigma_{rp} = S_\epsilon E_{rp} E_{rm}^{-1} \sigma_{rm}$
Reinforcement Modulus	FL^{-2}	E_{rp}	$E_{rp} = S_\sigma E_{rm}$	$E_{rp} = S_\sigma S_\epsilon^{-1} E_{rm}$
Poisson's Ratio		ν_p	$\nu_p = \nu_m$	$\nu_p = \nu_m$
Mass Density	FL^{-3}	ρ_p	$\rho_p = S_\sigma S_\ell^{-1} \rho_m$	$\rho_p = S_\sigma S_\ell^{-1} \rho_m$
Concentrated Load	F	P	$P_p = S_\sigma S_\ell^2 P_m$	$P_p = S_\sigma S_\ell^2 P_m$
Pressure	FL^{-2}	P	$P_p = S_\sigma P_m$	$P_p = S_\sigma P_m$
Moment	FL	M	$M_p = S_\sigma S_\ell^3 M_m$	$M_p = S_\sigma S_\ell^3 M_m$



Materials Similitude for the Case
 $E_{rp}/E_{rm} \neq S_\sigma/S_\epsilon$

FIGURE 2. EXAMPLES OF STRESS VS STRAIN PLOTS RESULTING IN DISTORTED MODELS

SECTION III

LITERATURE REVIEW

A. MODEL CONCRETE

The selection of suitable materials to model concrete requires the selection of an aggregate and a cementitious material, and the relative quantities of those plus water to model accurately the properties of the prototype.

Desirable aggregate used in concrete are of angular shape to provide maximum surface area for cement coating, and to augment particle interlocking.

The maximum size of aggregate permitted by ACI (Reference 5) is governed by the clearance between sides of forms and adjacent reinforcing bars. Size of aggregates may not exceed one-fifth of the narrowest dimension between sides of forms, one-third of the depth of the slabs, nor three-fourths of the minimum clear spacing between individual reinforcing bars.

Geometric scaling, S_g , of the gradation curve is desirable for the model to meet geometric similitude requirements. In the past, microconcrete researchers have shied away from scaling the finer aggregates. Large amounts of aggregates finer than the No. 100 to No. 200 sieves have been found to require extremely large quantities of water resulting in excessive air voids, thus seriously influencing the mechanical properties of the model concrete (Reference 6). Historically, attempts to model the aggregate size have merely been to

reduce the largest particles to the size that meets the requirements of ACI. The remaining portion of the gradation curve, which was made up of smaller particles, was left at the original gradation causing the curve for the model aggregate to become very steep and uniform. However, it has been found that it is the amount of aggregate, and not the gradation, that has the greatest effect on the mechanical properties of model concrete.

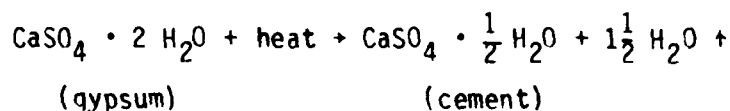
The gradation does have some effect, in that inconsistent grading between batches may cause significant strength variations (Reference 7). Mirza (Reference 7) experimented with several trial mixes using a local sand with the only restriction that it pass a certain sieve. One-hundred specimens were tested in compression and variation in strength were noted for the same water/cement and aggregate/cement ratios. These variations were eventually traced to inconsistent grading of the sand from batch to batch. Therefore, although the quantity of aggregates has the greatest affect on the strength, the gradation should be controlled.

Cementitious materials used thus far in concrete modelling are Portland cement and gypsum plaster. Portland cement of the Type I, normal, and Type III, high early strength, commonly used in prototype concrete, have also been popular in one-half to one-tenth scale models. Due to the relatively large size of the cement particles, obvious problems exist when trying to model in the 1/60 to 1/90 size. The cement particles are as large as a major portion of the geometrically scaled aggregate. Furthermore, the attractiveness of using Portland cement is diminished considering that Portland cement requires 10 to 28 days to develop the required stable strength level. Severe shrinkage problems are often associated with the use of Portland

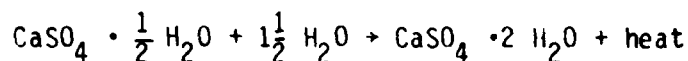
cement which is an intolerable condition in super-small scale modelling where wall thicknesses may be as small as a fraction of an inch. Another disadvantage of using Portland cement is that excessive strength variation associated with changes in specimen size has been found with Portland cement mortars (Reference 8). Generally, increased tensile strengths occur with a reduction in specimen size.

In 1967, Sabnis and White (Reference 8) began looking for an alternative bonding agent. Their studies led to the investigation of gypsum plaster. Since then, limited research has been continued mainly at the University of California, Berkeley and Cornell University, New York.

Gypsum cement originates from raw gypsum. The basic mineral is ground and calcined to produce a powder with uniform chemical and physical properties. The calcination process removes a portion of the chemically combined water in the following reaction:



Since the reaction is reversible, adding water to the gypsum cement forms gypsum once again, as follows:



Gypsum cement differs from gypsum plaster in the size and the shape of the crystals formed during the manufacturing process. The gypsum cement crystals require a smaller quantity of water to complete the reverse reaction, and thus result in a harder, stronger, and denser finished product.

There are three main reasons for gypsum cement's superiority over Portland cement in super small scale modelling: 1) Rapid curing time, 2) small particle size, and 3) low distortion. Gypsum cures rapidly and can actually be removed from its forms within 30 to 60 minutes after mixing. In fact, gypsum gains strength and stiffness by drying, and will become too brittle if allowed to air dry for a period of several days or longer.

The clay size particles of gypsum do not interfere with the role of the microaggregate.

Gypsum cement exhibits very low distortion upon curing. Unlike Portland cement mortars which contract; gypsum mortars expand. Maximum expansion for pure gypsum cement excluding aggregate is 0.080 percent. No other cementitious material exhibits such a low distortion. With the addition of microaggregate, expansion is even further minimized.

Gypsum cement is slightly soluble, amounting to about two grams per liter of water. This slight solubility is handy for cleanup after mixing and pouring.

Gypsum is also safe to work with. It is nontoxic, nonallergenic, odorless, and nondermatitic. It is noncorrosive and noncombustible, and, with a pH of 6.5 to 7.5, has a virtually neutral reaction.

Gypsum has been found to be compatible with a wide variety of chemicals, powders, and granular materials. However, gypsum crystals do not readily bond to aggregates larger than No. 10 mesh.

The water used in mixing should be low in contaminants. If it is drinkable, it is suitable for mixing. United States Gypsum recommends water between 70° and 100°F, the temperature range in which gypsum has its maximum solubility.

Two types of gypsum cements used previously in modelling are Ultracal® 30 and Ultracal® 60, manufactured by United States Gypsum. The number is based on the approximate amount of time in minutes required for set before the forms can be removed.

Ultracal® 30 has high surface hardness and compressive strength, and sets quickly. It is commonly used in industry and is the more readily available of the two.

Ultracal® 60 is similar to Ultracal® 30 except that its slightly higher consistency gives it less surface hardness and compressive strength. In addition, the longer set gives it less expansion.

The following are properties of pure Ultracal®, as supplied by the manufacturers and presented here for comparison of the two cements:

	Use Consistency (Part of water by weight per 100 parts of plaster)	Hand Mix Vicat Set (minutes)	Strength at	Setting		Surface Hardness
			Use Consistency Minimum Dry Compressive	Expansion % FINAL	MAX	
Ultracal® 30	38	25-30	6,000	0.60	0.80	115
Ultracal® 60	39	75-90	5,000	0.55	0.65	105

Additives are available which retard the rate of setting. United States Gypsum recommends a sodate retarder. Retarders reduce the strength of the cement but may be necessary for use with intricate modelling. Figure 3 is a guide for the use of a sodate retarder.

Gypsum mortars, consisting of gypsum, sand, and water have been used to model concrete as small as the 1/20 scale size. While this scale is quite a bit larger than the scale required in this project, past studies warrant review.

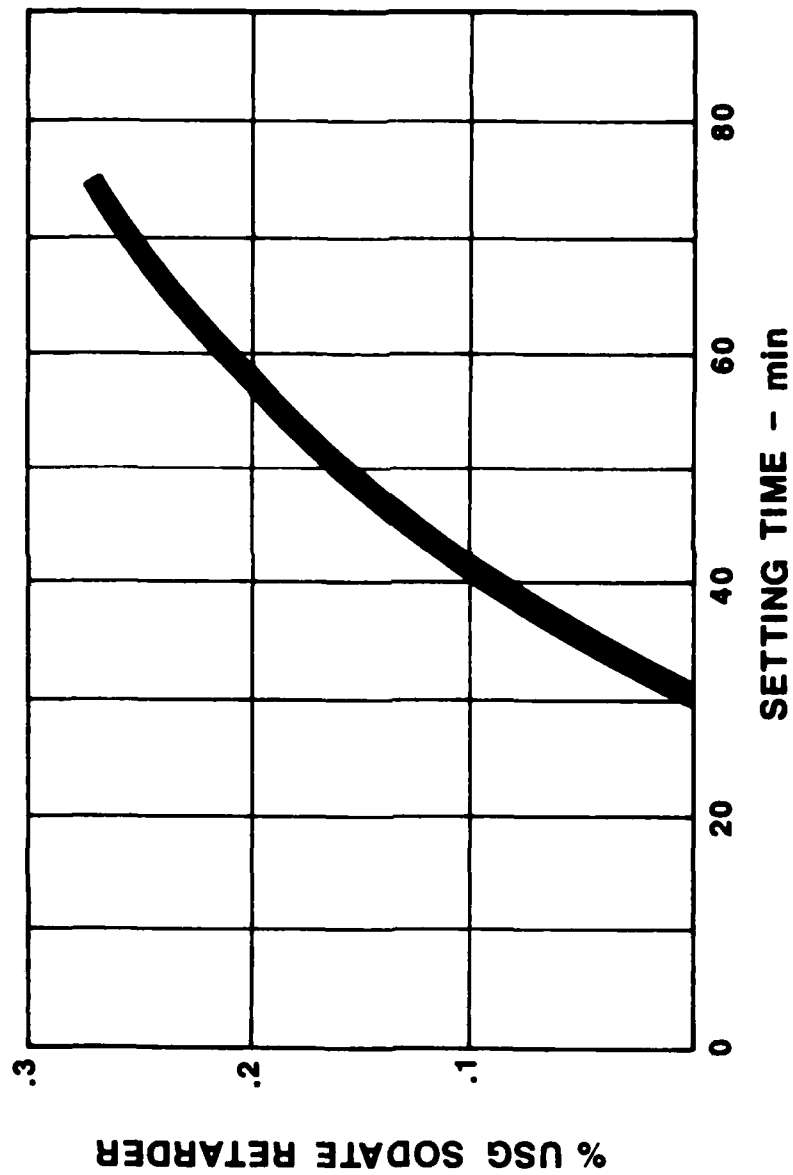


FIGURE 3. APPROXIMATE RETARDING EFFECT OF USG SODATE RETARDER ON MOLDING, CASTING OR/POTTERY PLASTERS

(From United States Gypsum)

The addition of aggregate to the gypsum makes the mix similar to concrete. This is especially evident in the effects on tensile strength. The ratio of compressive strength to tensile strength for pure gypsum is much higher than for concrete. The addition of aggregate lowers the tensile strength.

The effects of varying the water/gypsum cement ratio and the aggregate/gypsum ratio as obtained by Sabnis and White (Reference 8), are shown in Figures 4 and 5, where the compressive strength is plotted against the ratios. It is evident that the addition of both water and aggregate lowers the compressive strength. It should also be remembered that water in excess of the amount required to complete the reaction with the plaster will be removed by the drying process, resulting in air voids.

Gypsum mortars develop strength rapidly. This is a potential problem since tests must be run at specific times after pouring, when the micro-concrete has developed the desired strength. Also, the model may gain strength during prolonged testing. This problem can be alleviated by sealing the moisture in the mix at the desired strength level. Sikaseal, Thoroclear, and ordinary shellac have been found to be effective sealants. The strength-age relations for various mixes are shown in Figure 6. It is evident that the age of gypsum mortars becomes a less critical factor when the specimens are sealed.

The uniaxial compressive stress strain characteristics of gypsum mortars have been shown to be similar to those of concrete. The most detailed research has been done by Kandasamy (Reference 9).

The effect of specimen size on strengths of gypsum mortars is summarized by Mirza (Reference 10).

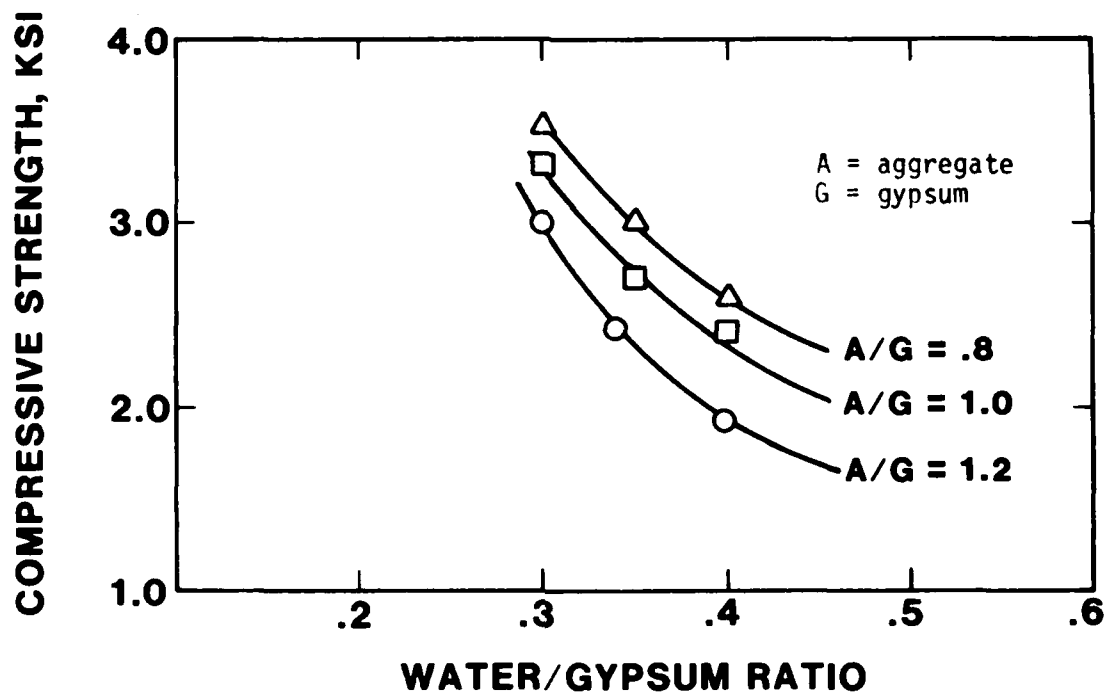


FIGURE 4. EFFECT OF WATER-GYPSUM RATIO ON f'_c
(FROM REFERENCE 8)

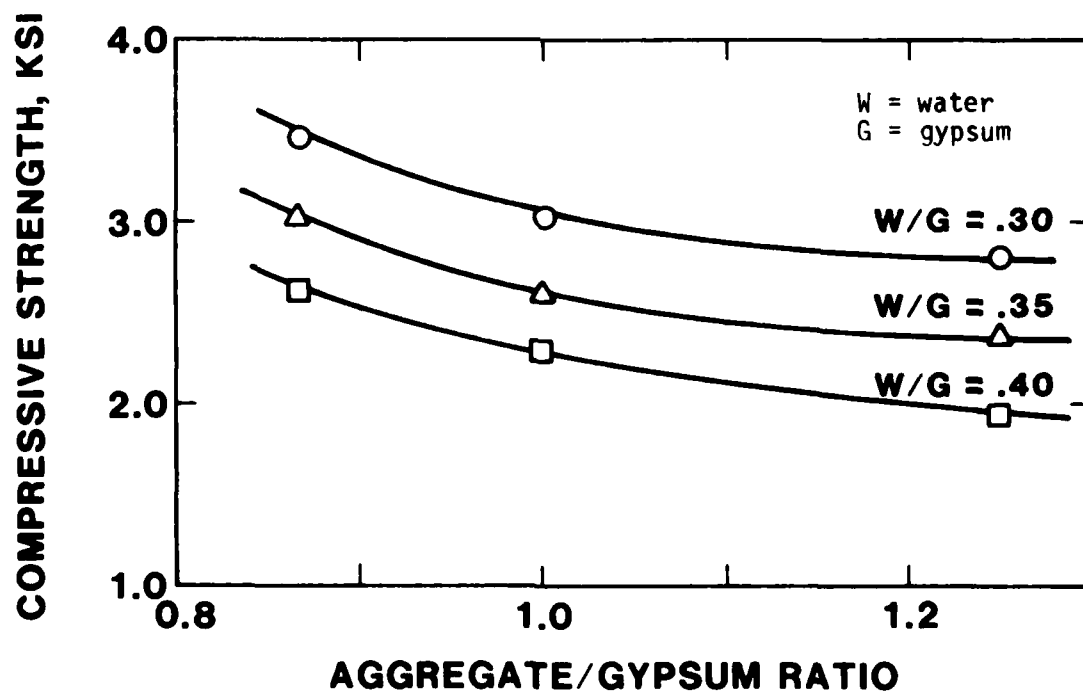
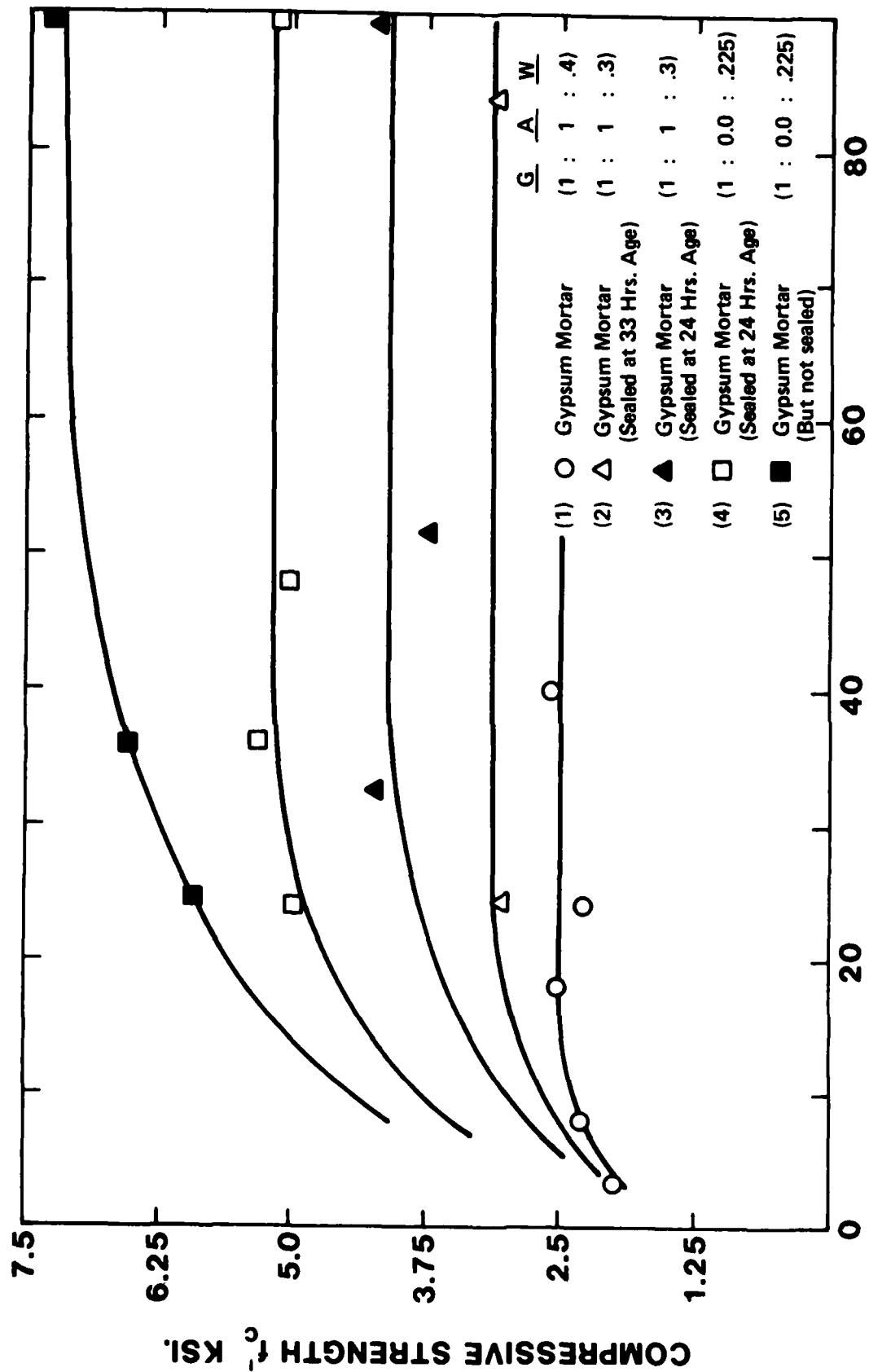


FIGURE 5. EFFECT OF AGGREGATE CONCENTRATION ON f'_c
(FROM REFERENCE 8)



AGE FOR GYPSUM MORTAR, HR

FIGURE 6. STRENGTH-AGE RELATIONS FOR GYPSUM MORTARS
(FROM REFERENCE 8)

1. The amount of moisture present in different size specimens is by far the most important parameter in observed size effects.
2. With proper surface sealing techniques for control of moisture, there is negligible size effect in compressive strength of cylinders ranging in size from 0.5 by 1 inches to 3 by 6 inches.
3. Using the same sealing procedures as for compression tests, the modulus of rupture values for beams ranging from one-half inch to three inches deep exhibited a size effect.
4. Coated split-tensile specimens showed no discernible size effects when material density and moisture content were identical.

Sabnis and White (Reference 8) report that unsealed specimens gave an increase in strength of about 50 percent as specimen diameter decreased from three to one-half inch while surface sealed cylinders gave no measurable size effect. Their findings indicate that one-half inch deep beams were only ten percent stronger than three inch beams in rupture and therefore, the size effect could be considered insignificant. It was concluded that for smaller specimens, a gypsum microconcrete should give better results than a Portland cement microconcrete because the sealing process eliminates most of the size effects.

B. MODEL REINFORCEMENT

The similitude conditions for a true model with no distortion (see Table 1) require that the stress-strain properties of the model reinforcement be geometrically similar to that of the prototype reinforcing.

The characteristics to be considered for the reinforcement include:

1. Yield strength
2. Shape of stress-strain curve
3. Bond characteristics between reinforcement and microconcrete.

The suitability of several prospective materials for micro-reinforcement, including metals, plastics, and glass fibers, has been investigated (Reference 11). The low- and medium-carbon steels used for conventional reinforcement have fairly well-pronounced yield points and yield plateaus with large ductility. The model material should have the same characteristics. The only material known to exhibit such characteristics, aside from steel itself, is phosphor bronze.

If steel is used as the model reinforcement, equality of the modulus of elasticity of the model and prototype is automatically satisfied; S_E is unity. Equality of yield points have even been achieved through a process of controlled annealing. However, material properties including yield point, are susceptible to gross variations caused by the heating process, as the effects are magnified due to inconsistencies of the model reinforcement (i.e., cross-sectional area, chemical inconsistency).

Various techniques have been used in attempting to model the surface deformations of prototype reinforcement. Included are sand coating (held in place by shellac), rusting, threading, and cold deforming of wires.

Adequate bond has been achieved by the rusting of plain wires; however, it is recommended that rusted wires not be used because variability of bond strength is high (Reference 12).

Successful bond strength has been achieved with commercially threaded wire such as that used for bicycle spokes. Unfortunately, attempts to procure threaded wire in the small sizes required for 1/60 and 1/90 scale modelling were unsuccessful.

Although adequate ultimate bond strength has been achieved in some cases between plain wire and plaster, the steel concrete bond of prototype reinforced concrete is a combined effect of adhesion and friction. Hence with plain wires only the friction component is developed, therefore, a marked decrease in ultimate bond stress occurs with increasing imbedment ratio (length/diameter).

A technique was developed in the Cornell Structural Models Laboratory to cold-deform wire. The desired deformations are obtained by passing the wire through two pairs of perpendicular knurls, continuously deforming the length of wire. Further research in Japan by Murayama and Noda (Reference 13) using Cornell's deforming techniques, revealed that wires inwardly deformed to the same scaled dimensions (S_d) as the raised lugs of the prototype reinforcement, best modelled the characteristics of the prototype. Adhesion is developed in the deformations, as they serve as microconcrete keys. The bond decreases gradually as the material around the deformations is fractured during pull-out. Harris, Sabnis, and White (Reference 12) concluded that laboratory deformed wires are comparable to prototype deformed bars with respect to bond strength in direct pull-out.

Cold deforming increases the yield strength of the wire. Annealing has the opposite effect, with yield strength inversely proportional to annealing duration and temperature. Neither cold-deforming nor annealing have an effect on the modulus of elasticity (see Figure 7, Reference 7).

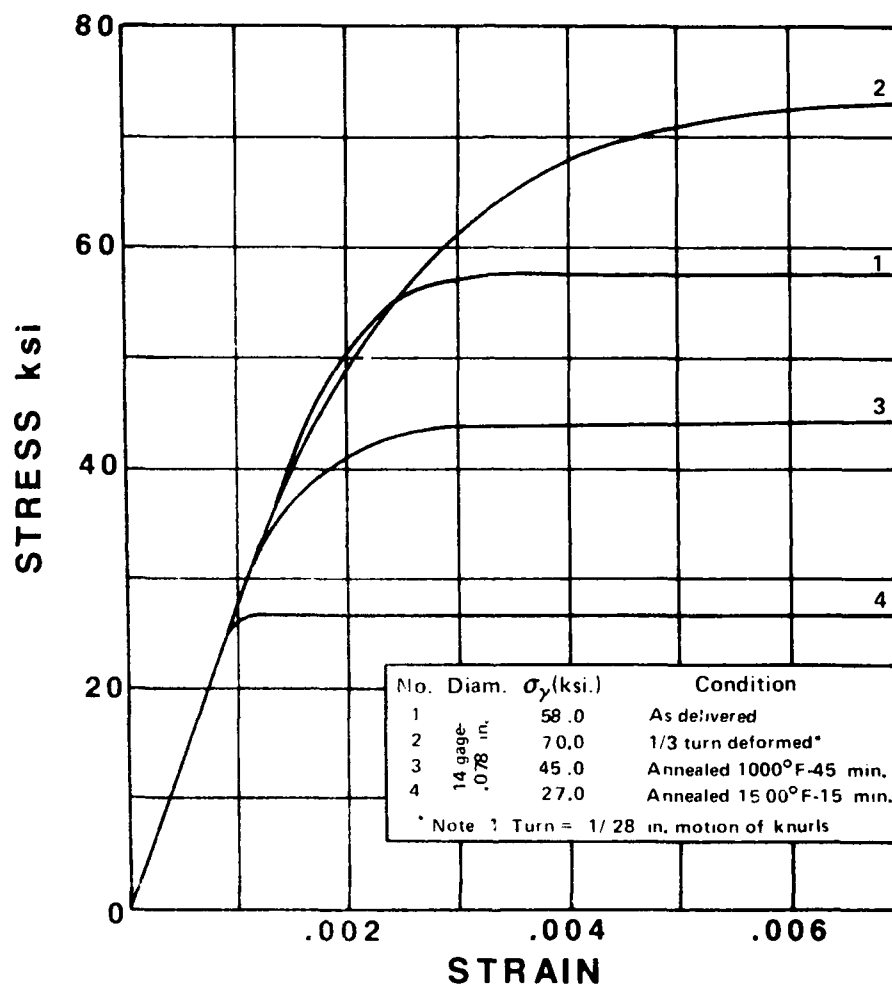


FIGURE 7. EFFECT OF DEFORMATION AND HEAT TREATMENT ON STRESS-STRAIN BEHAVIOR OF REINFORCING WIRE

(From Reference 7)

SECTION IV

DEVELOPMENT OF MICROCONCRETE MIX

The following properties and characteristics were considered in the development of the microconcrete mix:

1. Aggregate shape, scaling, and gradation
2. Water/Cement/Aggregate ratio
3. Compressive strength
4. Tensile strength
5. Modulus of Elasticity
6. Modulus of Rupture
7. Workability

The design approach was to first scale the aggregate and then mix batches of differing water/cement/aggregate ratios, testing each mix after curing for compressive strength. It was surmized that after having developed adequate compressive strength as a starting point, the mix could then be adjusted, if need be, to develop the necessary properties and characteristics.

An infinite number of variations in the mix could be achieved by changing the water/cement ratio, the water/aggregate ratio, the type and gradation of aggregate, and the type of cementing agent. Previous research by Chawdbury, White, and Scott (Reference 4), six trial mixes, and Mirza (Reference 10), one trial mix, served as a starting point for the design of the water/cement/aggregate ratios, although their mixes utilized larger aggregate.

A medium- to fine-grained clean sand was chosen for the micro-aggregate. The sand, referred to as Edgar sand, was mined from Edgar, Florida. Viewed under a microscope, the particles can be seen to fall into classes A and B, shown in Figure 8. Classified as subangular to angular, Edgar sand simulates desirable prototype concrete aggregates.

The microaggregate was scaled from No. 2 concrete aggregate (Reference 14). It was first scaled at $S_g = 1/150$, corresponding to the necessary model size to fit the entire structure into the centrifuge bucket. Mix No's 1¹-1-.30, 1²-1-.25, 1³-.8-.25 and 1⁴-.9-.25 were tried using this gradation with a maximum particle size of 0.297mm. Adequate compressive strength combined with suitable workability was not achieved (Table 2). To increase the compressive strength, the maximum particle size was increased to 0.595mm. An increase in compressive strength was achieved with this gradation for identical water/cement/aggregate ratios (i.e., compare trial mixes 1⁵-.8-.25 and 1³-.8-.25, Table 2). This gradation was held constant for the rest of the experiment and was incorporated into the final mix design. The gradation was distorted from the $S_g = 1/150$ scaling due to the excessive size of the largest particle. However, when the model scale was later increased to 1/60 and 1/90 scale due to the nonfeasibility of physical modelling at the 1/150 scale (see Section VII), the final gradation happened to fall within the proper scale.

Figure 9 shows the boundary gradation curves for the No. 2 concrete aggregate and the gradation curve for the microaggregate.

Gypsum cement was chosen as the cementing agent because of its rapid curing time, small particle size and low distortion. Specifically, Ultracal 100, manufactured by United States Gypsum, was

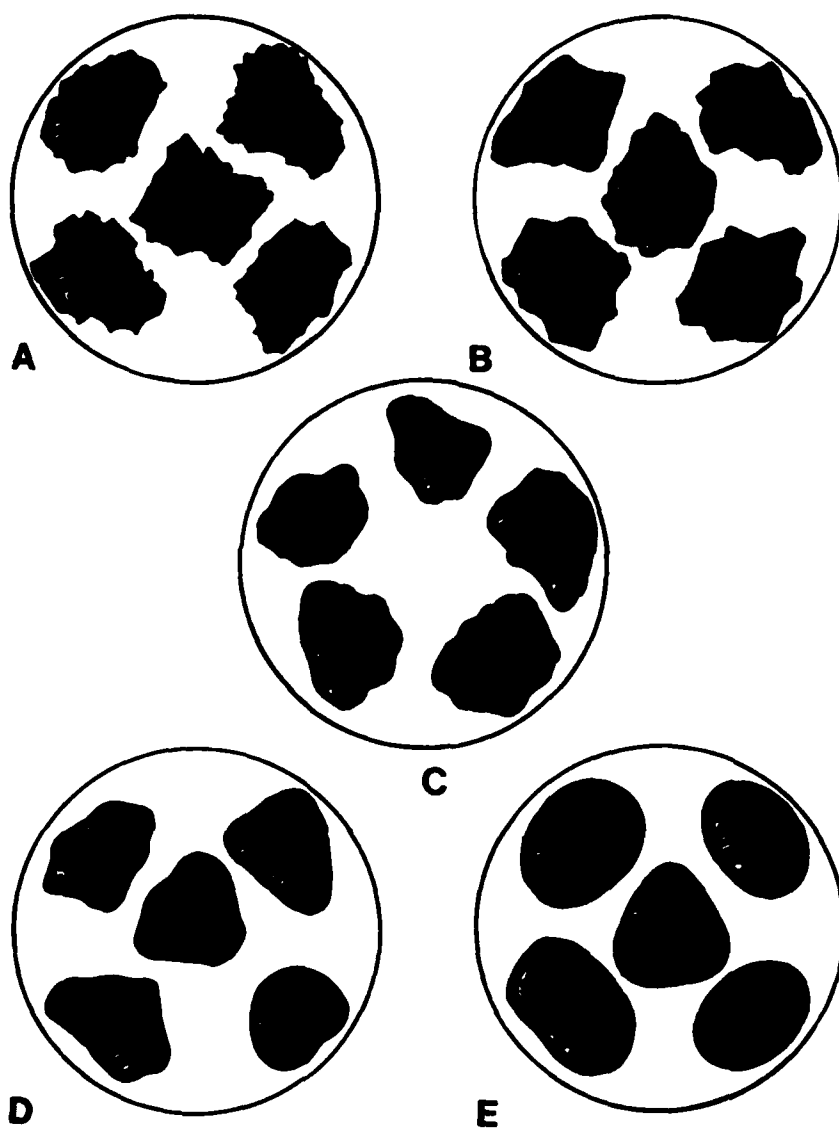


FIGURE 8. CHART TO SHOW AGGREGATE ROUNDNESS CLASSES. A, ANGULAR; B, SUBANGULAR; C, SUBROUNDED; D, ROUNDED; E, WELL-ROUNDED

TABLE 2. RESULTS OF COMPRESSION TESTS FOR VARIOUS TRIAL MIXES

MIX NO.		AGE AT TESTING (hr.)	MAX LOAD (kips)	AREA* (in ²)	MAX COMPRESSIVE STGTH (psi)	ACTUAL LENGTH (in.)	WEIGHT (lbs)	UNIT WEIGHT (lb/ft ³)	WORK-ABILITY RATING
1 ¹ -1-.30	#1	1	20.4	7.069	2886				Fair
	#2	2	23.9	7.069	3381				
	#3	24	22.2	7.069	3141				
	#4	48	23.5	7.069	3324				
1 ² -1-.25	#1	1	5.8	7.187	807	6.02			Poor
	#2	1	16.8	7.187	2338	6.07			
	#3	2	24.1	7.187	3353	6.06			
	#4	2	27.4	7.187	3812	6.07			
	#5	24	26.4	7.187	3673	5.98			
	#6	24	30.4	7.187	4230	6.06			
	#7	48	31.6	7.187	4397	6.08			
	#8	48	32.3	7.187	4494	6.06			
1 ³ -.8-.25	#1	1	8.5	7.187	1183	6.05			Fair to Good
	#2	1	11.7	7.187	1628	6.05			
	#3	2	17.8	7.187	2477	6.10			
	#4	2	24.6	7.187	3423	6.08			
	#5	24	28.4	7.069	4018	6.00			
	#6	24	23.3	7.069	4004	5.95			
	#7	24	28.3	7.187	3938	6.06			
1 ⁴ -.9-.25	#1	24	21.9	7.120	3075	5.86	3.135	129.8	Poor to Fair
	#2	24	26.7	7.120	3750	5.91	3.136	128.8	
	#3	24	26.0	7.120	3652	5.89	3.132	129.0	
	#4	24	22.9	7.120	3216	5.89	3.137	129.2	
	#5	48	27.4	7.120	3848	5.89	3.145	129.6	
	#6	48	24.3	7.120	3483	5.90	3.140	129.2	
	#7	48	24.7	7.120	3371	5.89	3.138	129.3	
	#8	48	26.3	7.120	3694	5.89	3.141	129.4	
1 ⁵ -.8-.25	#1	24	31.3	7.120	4390	5.83	3.148	130.9	Good
	#2	24	32.8	7.120	4607	5.80	3.127	130.8	
	#3	24	30.6	7.120	4298	5.86	3.148	130.4	
	#4	48	29.8	7.120	4135	5.84	3.119	129.6	
	#5	48	28.3	7.120	3975	5.84	3.125	129.9	
	#6	48	32.8	7.120	4581	5.83	3.139	130.7	
	#7	48		7.120		5.87	3.134	129.6	
	#8	48		7.120		5.85	3.118	129.4	
1 ⁶ -1-.25	#1	24	23.4	7.120	3226	5.81	3.120	130.3	Poor (many voids)
	#2	24	21.6	7.120	3034	5.81	3.106	129.7	
	#3	24	25.4	7.120	3226	5.84	3.112	129.3	
	#4	48	24.7	7.120	3290	5.81	3.117	130.2	

* Nominal 3-inch diameter by 6-inch height.

TABLE 2 (continued)

MIX NO.	AGE AT TESTING (hr.)	MAX LOAD (kips)	AREA* (in ²)	MAX COMPRESSIVE STGTH (psi)	ACTUAL LENGTH (in.)	WEIGHT (lbs)	UNIT WEIGHT (lb/ft ³)	WORK-ABILITY RATING
1 ⁷ -.4-.20	#1	24	27.7	7.120	3469	5.91	3.129	128.5
	#2	24	23.1	7.187	3214	5.89	3.137	128.0
	#3	24	19.8	7.187	2755	5.95	3.131	126.5
	#4	24	24.2	7.120	3399	5.95	3.127	127.5
	#5	48	28.7	7.187	3993	5.95	3.128	126.4
	#6	48	24.8	7.187	3451	5.89	3.121	127.4
	#7	48	26.5	7.187	3677	5.84	3.126	128.7
1 ⁸ -.7-.25	#1	24	28.7	7.120	4031	5.84	3.131	130.1
	#2	24	26.8	7.120	3764	5.86	3.142	130.1
	#3	48	30.5	7.120	4284	5.80	3.109	130.0
	#4	48	29.1	7.120	4087	5.87	3.128	129.3
	#5	48	27.7	7.120	3890	5.86	3.124	129.4

Trial Mix No. Designations:

A^N-B-C

A = Part Gypsum Cement by Weight

B = Part Aggregate by Weight

C = Part Water by Weight

N = Chronological Sequence Number

GRADATION CHART

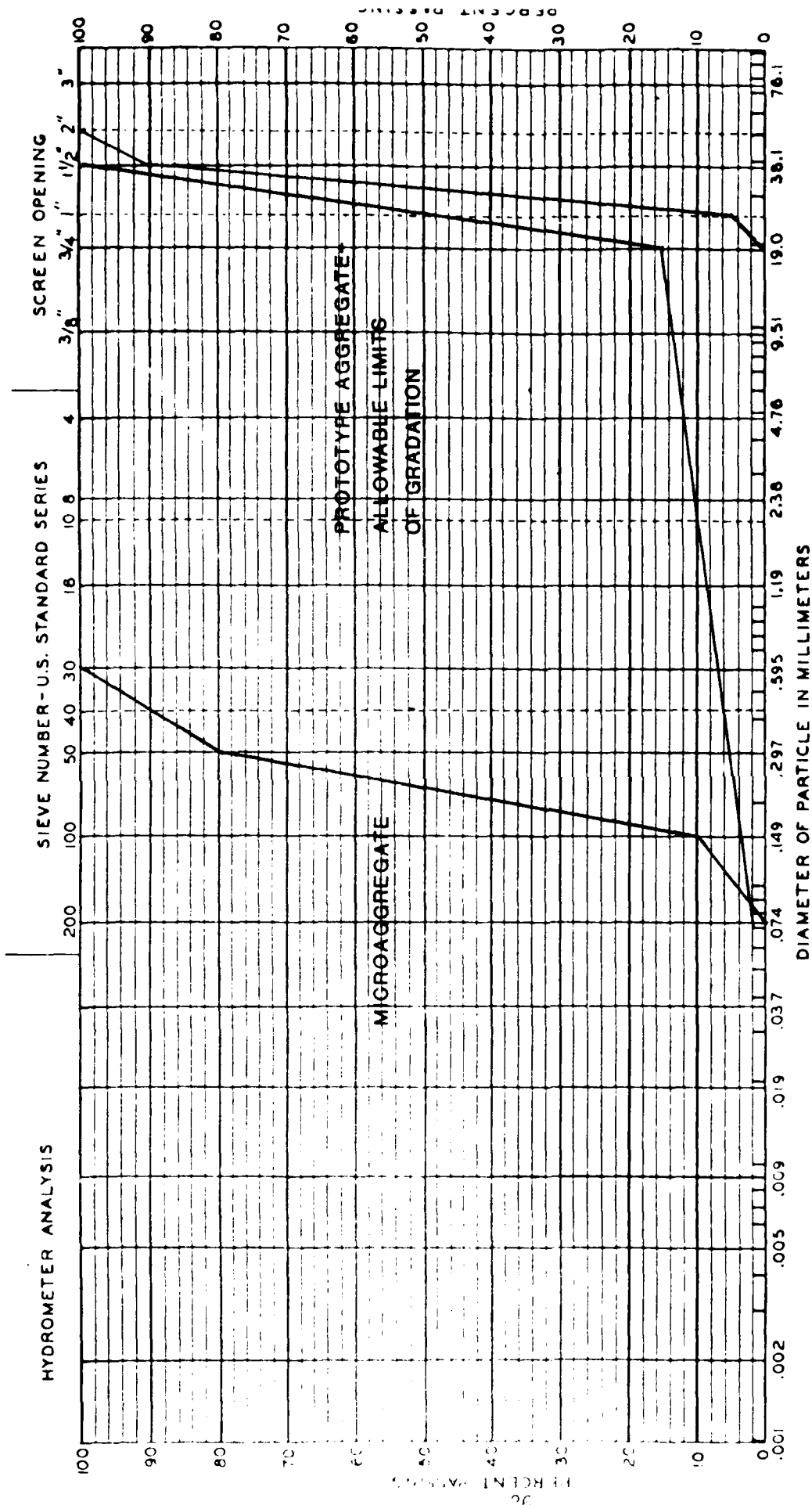


FIGURE 9. AGGREGATE GRADATION CURVES FOR PROTOTYPE AND MODEL

chosen over Ultracal® 30 for its longer set time and smaller degree of expansion.

Eight mixes were tried. Each design was based on the results of the previous design. Batches were prepared, and three-inch by six-inch cylinders were poured as described in Appendix A. Cylinders were broken in uniaxial compression on the University of Florida's Tinius Olsen testing machine, model 400,000 lb, Super "L." Tests were run in accordance with the Standard Test Method for Compressive Strength of Cylindrical Concrete Specimens, ASTM Designation: C39-81.

The results of the compressive tests, along with the workability ratings for the trial mixes, are tabulated in Table 2. The workability rating was given as a qualitative measure of the base at which the microconcrete was mixed, placed, and vibrated. Mix No. 1⁵-.8-.25 was chosen for further testing due to its relatively high compressive strength, good workability characteristics and relatively high concentration of aggregate (compared to Mix No. 1⁸-.7-.25).

The next step was to determine the modulus of elasticity of the microconcrete in compression loading. It is critical in the development of a true model that the scaling factor for the modulus of elasticity, S_{E_c} , equals unity.

Four 3-inch by 6-inch cylindrical specimens were prepared. Forty-eight hours after pouring, the cylinders were sealed with shellac to prevent further drying, thus holding constant the material properties. The cylinders were then instrumented with SR-4 strain gages. Strain was measured at 1 kip load increments. One test cylinder was thrown out due to failure of the strain gage connection. The other three tests yielded useful data. The load-strain curves are plotted in Figure 10. The

secant moduli at $0.5f'_c$ were 3,000,000 psi, 3,600,000 psi, and 3,100,000 psi, corresponding to ultimate compressive strengths of 4300 psi, 4400 psi and 4100 psi, respectively.

The modulus of elasticity of concrete varies with density and strength. ACI predicts the modulus of elasticity with the following equation:

$$E_c = \omega^{1.5} 33\sqrt{f'_c}$$

where, E_c = modulus of elasticity

ω = density of concrete

f'_c = strength in compression

For comparison, values of the moduli of normal weight concrete (145 lb/ft^3) for typical compressive strengths are:

<u>f'_c (psi)</u>	<u>E_c (psi)</u>
3000	3,150,000
3500	3,400,000
4000	3,640,000
4500	3,860,000
5000	4,070,000

The moduli of the microconcrete ($E_c=3,300,000$ psi for $f'_c=4085$ psi) are close to these values.

Using the density of the microconcrete (130 lb/ft^3), the ACI equation predicts the results of the stress-strain tests. The density of the microconcrete is within ten percent of the density of the prototype concrete.

Next, the tensile strength of the microconcrete was determined by the split-cylinder test. Testing was performed in accordance with the ASTM Standard Test Method for Splitting Tensile Strength of Cylindrical Concrete Specimens, Designation: C496-71. In this test, a cast cylinder is placed on its side so that the compression load P is applied

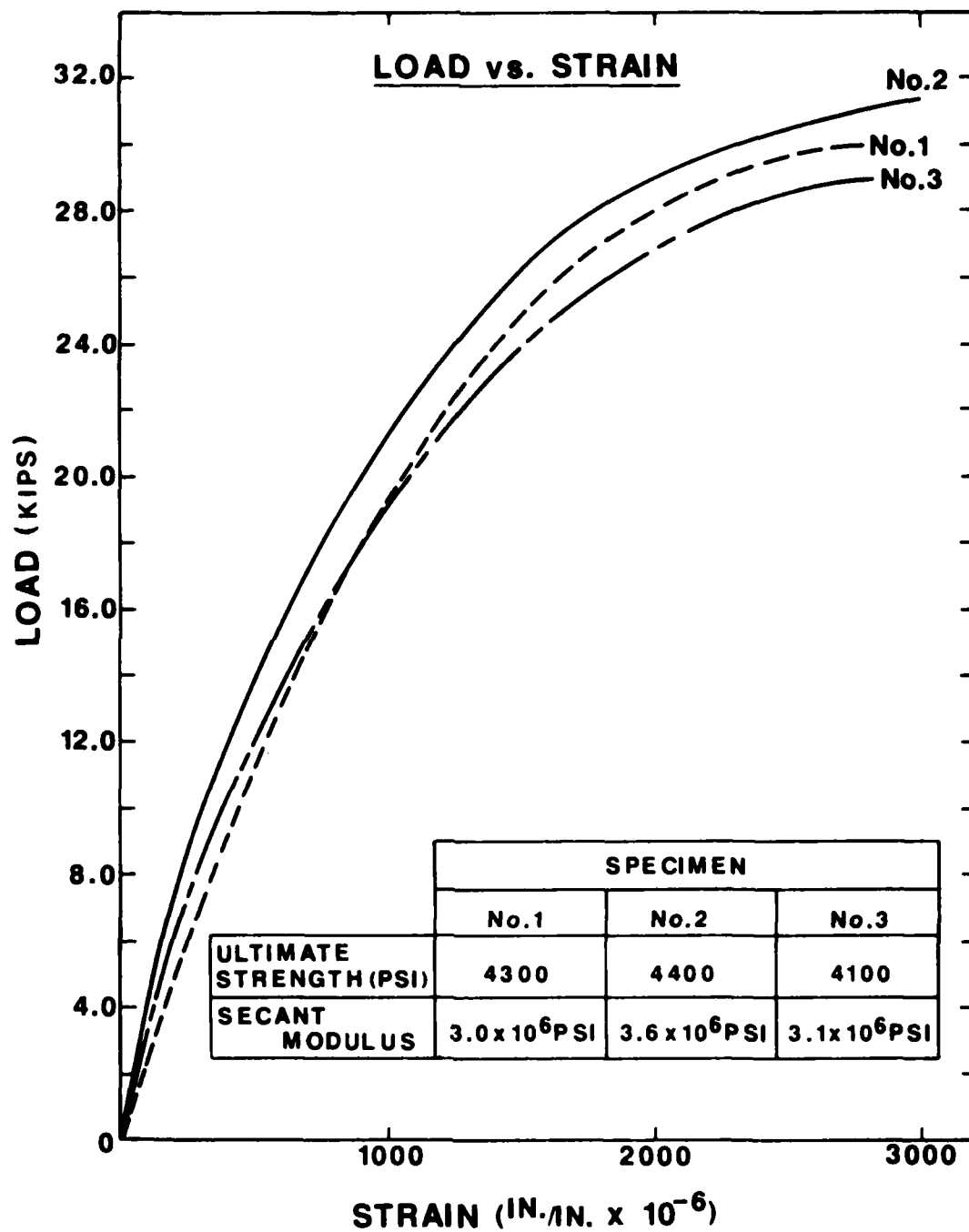


FIGURE 10. COMPRESSION LOAD VERSUS STRAIN FOR MICROCONCRETE

uniformly along the length of the cylinder in the direction of the diameter. The cylinder splits in half when the tensile strength is reached. Based on the theory of elasticity for a homogeneous material in a biaxial state of stress, the tensile stress equation follows:

$$\text{Stress } (f_{c_t}) = \frac{2P}{\pi(\text{diameter})(\text{length})}$$

The ACI Code (Reference 5) states that the tensile strength of concrete is a more variable property than compressive strength, ranging from ten to fifteen percent of it. The ACI Code provides the following relationships between the compressive and tensile strengths for various types of concretes.

$$\text{normal weight concrete } f_{c_t} = 6.7\sqrt{f'_c}$$

$$\text{sand-lightweight concrete } f_{c_t} = 5.7\sqrt{f'_c}$$

$$\text{all-lightweight concrete } f_{c_t} = 5\sqrt{f'_c}$$

As in the compression tests, 3-inch by 6-inch microconcrete cylinders were tested. Cylinders were coated with shellac after curing for 48 hours. The load was applied with the Tinius Olsen testing machine. The results of the eight split tensile tests are shown in Table 3. As is the case with normal concrete, variation in the tensile strength was noted. The individual results were not excessively greater than or less than the expected tensile strength of the prototype concrete, although the average tensile strength of 327 psf was slightly less than the value by the ACI Code.

Tests were also performed on the microconcrete to determine the modulus of rupture, f_r , or the tensile strength in flexure. In prototype concrete, the modulus of rupture gives higher values for tensile strength than the split cylinder test. The ACI Code states that

TABLE 3. RESULTS OF MICROCONCRETE TENSILE TESTS FOR MIX 1⁵-.8-.25

		AGE AT TESTING (hr)	LENGTH (in)	DIAMETER (in)	MAX LOAD (kips)	MAXIMUM TENSILE STRENGTH* (psi)	VOLUME (ft ³)	WEIGHT (lb)	UNIT WEIGHT (lb/ft ³)
1 ⁵ -.8-.25	#1	48	5.85	3.005	7.75				
	#2	48	5.81	3.007	9.45				
	#3	48	5.84	3.003	6.80				
	#4	48**	5.84	3.005	12.41	450	.0240	3.121	130.2
	#5	48**	5.78	3.010	11.32	414	.0238	3.100	130.2
	#6	48**	5.82	3.006	8.99	327	.0239	3.123	130.6
	#7	48**	5.79	3.010	7.24	264	.0238	3.116	130.7
	#8	48**	5.91	3.010	8.06	288	.0243	3.162	129.9

* $f_{ct} = 2P/\pi (\text{dia})(\text{length})$

** shellaced at 48 hours; broken 4 days after coating

generally an average value for the modulus of rupture may be taken as $7.5\sqrt{f'_c}$.

The rupture testing was performed on 3- by 3- by 9-inch rectangular shaped beams. As with the microconcrete cylinders, the beams were one-half the size of the test specimens usually used for the prototype tests. Again, they were air cured for 48 hours, at which time they were coated with shellac to prevent further curing. The beams were simply supported, and the third-point loading method was employed to give the beams pure bending zones. The load was applied with the Tinius Olsen testing machine. Tests were run in accordance with the Standard Test Method for Flexural Strength of Concrete (using Simple Beam with Third-Point Loading) ASTM Designation: C78-84.

The results of six tests were (see Table 4):

TABLE 4. RESULTS OF MICROCONCRETE RUPTURE MODULUS TESTS

BEAM #	L (in)	b (in)	d (in)	P (lb)	f_r (psi)
1	9	3.1	3	1927	622
2	9	3	3	1794	598
3	9	3.1	3	1993	643
4	9	3.1	3	1917	618
5	9	3.05	3	1717	563
6	9	3.05	3	1724	565

where, $f_r = PL/bd^2$

P = Load at failure

L = Length

b = width

d = depth

The average value of the tests was twenty percent higher than the value predicted by the ACI code prototype concrete.

Additional compression tests were performed on Mix No. 1⁵-.8-.25 in conjunction with other tests (i.e., load deflection tests on reinforced beams). Ultimately, a total of 37 compression tests were run. The average compression strength was 4085 psi. Individual results are shown in Table 5 and show (A) sealing was able to control strength, i.e., no effect on strength due to curing time, (B) excellent reproducibility in achieving equal densities when forming specimens, and (C) a standard deviation of 406 in strength among specimens.

Summary of properties of final Mix No. 1⁵-.8-.25

Compressive Strength = 4085 psi

Tensile Strength = 327 psi

Modulus of Elasticity = 3.3×10^6 psi

Modulus of Rupture = 601 psi

Unit Weight: 130 pcf

Workability Rating: Good

TABLE 5. RESULTS OF ADDITIONAL COMPRESSION TESTS PERFORMED ON MIX 1⁵-.8-.25

CYL SIZE (in)	COAT TIME (hrs)	TIME TESTED AFTER COAT (days)	ACT. LENGTH (in)	ACT. AREA (in ²)	WEIGHT (lbs)	UNIT WT. (pcf)	MAXIMUM LOAD (KIPS)	MAXIMUM COMPRESSIVE STRENGTH (psi)
3x6	24	9	5.88	7.12	3.096	127.8	24.83	3500
3x6	48	8	5.92	7.12	3.138	128.6	24.00	3400
2x4	24	9	4.04	3.16	.956	129.4	13.16	4150
2x4	24	9	4.07	3.17	.949	127.1	13.10	4150
3x6	48	8	5.84	7.11	3.127	130.1	28.45	4000
3x6	48	8	5.85	7.12	3.138	130.2	27.97	3950
3x6	48	8	5.78	7.12	3.148	132.2	30.40	4250
3x6	48	8	5.88	7.12	3.175	131.0	32.04	4500
2x4	48	8	3.98	3.16	.973	133.6	13.49	4250
2x4	48	8	3.99	3.16	.968	132.7	14.72	4650
3x6	48	1	5.85	7.12	3.158	131.0	26.37	3700
3x6	48	1	5.82	7.12	3.108	129.6	28.96	4050
3x6	48	1	5.85	7.11	3.105	129.0	29.20	4100
3x6	48	1	5.89	7.10	3.137	129.6	28.87	4050
3x6	48	1	5.81	7.11	3.132	131.0	30.50	4300
3x6	48	1	5.87	7.12	3.162	130.7	29.80	4200
3x6	48	1	5.85	7.12	3.144	130.4	31.71	4450
3x6	48	1	5.85	7.13	3.146	130.3	31.05	4350
3x6	48	1	5.89	7.10	3.151	130.2	25.79	3600
3x6	48	1	5.89	7.11	3.153	130.8	31.63	4450
3x6	48	1	5.86	7.10	1.137	130.3	35.41	5000
3x6	48	3	5.83	7.13	3.146	130.8	29.68	4163
3x6	48	7	5.83	7.12	3.106	129.3	30.49	4300
3x6	48	7	5.86	7.12	3.120	129.2	31.39	4400
3x6	48	7	5.81	7.12	3.107	129.3	29.10	4100
3x6	48	4	5.88	7.14	3.136	129.1	27.20	3390
3x6	48	4	5.83	7.14	3.109	129.1	27.21	3810
3x6	48	4	5.82	7.14	3.127	130.0	24.3	3400
3x6	48	2	5.81	7.10	3.119	130.6	25.2	3550
3x6	48	2	5.80	7.11	3.113	130.4	26.2	3680
3x6	48	2	5.80	7.10	3.120	130.9	23.4	3300

SECTION V

DEVELOPMENT OF MINIATURIZED REINFORCEMENT

The following properties and characteristics were considered in the development of the miniaturized reinforcements:

1. Yield strength
2. Modulus of Elasticity
3. Bond development

Black-annealed steel wire was chosen as the model reinforcement for several reasons. Since the material is steel, like the prototype reinforcement, it was expected to exhibit similar properties. Annealed steel wire was chosen because of its low yield strength (40 to 60 ksi) compared to nonannealed, cold rolled steel wire (80 to 100 ksi) which would have required the development of a tedious annealing procedure.

Black annealed steel wire is available in hardware stores where it is sold for use as tie and packaging wire. It is routinely manufactured in an assortment of diameters. The manufacturing process involves a cold rolling process of extruding it from bulk steel and an annealing process to lower its yield strength.

The miniaturized reinforcement was developed to model the steel reinforcement of the prototype structure. The prototype reinforcement consists of deformed bars of ASTM A615 billet steel of Grade 60, having a minimum specified yield stress of 60,000 psi. The Modulus of Elasticity of this type of steel is 29,000,000 psi. The deformations are in the form of protrusions, which serve to inhibit the longitudinal movement of the bar relative to the concrete.

Table 6 lists the ASTM designation A615-82 reinforcing bars by their bar designation numbers. The bar numbers are based on the number of eighths of an inch included in the nominal diameter of the bars. Included in Table 6 are some characteristics of the bars such as nominal weights, nominal dimensions, deformation requirements, and deformation-dimension ratios.

The prototype reinforcing bars are listed again in Table 7, along with their respective diameters and areas. Also listed are these respective diameters and areas reduced by the 1/60 and 1/90 model scale factors.

The miniaturized reinforcement was purchased locally and is distributed by the Anchor Wire Corporation of Goodlettsville, Tennessee. The three smallest diameter wires available were American Standard Wire Gauge sizes 28, 24, and 22 with corresponding diameters of .0162, .0230, and .0286 inch. The wire diameters are close to the 1/60 and the 1/90 scale diameters of the No. 8 and larger prototype reinforcement bars prevalent in the prototype structure. The 22- and 24-gauge wires are packaged in 117-foot length rolls; the 28-gauge is available in 100-foot length spools.

The first step in determining the suitability of the material was to determine its yield strength and modulus of elasticity, in tension. The best method found to perform the tensile testing was to hang a length of the wire from a rigid support and apply weights incrementally to the opposite end. The deformation was measured using a Gaertner M912 Horizontal-Vertical Cathetometer, accurate to .001 cm.

To perform the test, a sighting target line was marked as close as possible to the lower end of the wire. The Cathetometer telescope was

TABLE 6. DEFORMED BAR DESIGNATION NUMBERS, NOMINAL WEIGHTS,
NOMINAL DIMENSIONS AND DEFORMATION REQUIREMENTS

BAR DESIG- NATION NO.	NOMINAL DIMENSIONS ^a			DEFORMATION REQUIREMENTS, (in)			DEFORMATION-DIMENSION RATIOS			
	NOMINAL WEIGHT (lb/ft)	DIAMETER (in)	CROSS- SECTIONAL AREA (in ²)	PERI- METER (in)	MAXIMUM AVERAGE SPACING	MINIMUM AVERAGE HEIGHT	MAX. GAP (CHORD OF 12 1/8 OF NOMINAL PERIMETER)	MIN. HT. DIA.	HEIGHT AREA	HEIGHT PERI. DIAMETER
3	0.376	0.375	0.11	1.178	0.262	0.015	0.143	.0400	.1364	.0127
4	0.668	0.500	0.20	1.571	0.350	0.020	0.191	.0400	.1000	.0127
5	1.043	0.625	0.31	1.963	0.437	0.028	0.239	.0448	.0903	.0143
6	1.502	0.750	0.44	2.356	0.525	0.038	0.286	.0507	.0864	.0161
7	2.044	0.875	0.60	2.749	0.612	0.044	0.334	.0503	.0733	.0160
8	2.670	1.000	0.79	3.142	0.700	0.050	0.383	.0500	.0633	.0159
9	3.400	1.128	1.00	3.544	0.790	0.056	0.431	.0496	.0560	.0158
10	4.303	1.270	1.27	3.990	0.889	0.064	0.487	.0504	.0504	.0160
11	5.313	1.410	1.56	4.430	0.987	0.071	0.540	.0504	.0455	.0160
14	7.65	1.693	2.25	5.32	1.185	0.085	0.648	.0502	.0378	.0159
18	13.60	2.257	4.00	7.09	1.58	0.102	0.864	.045	.0255	.0144

a. The nominal dimensions of a deformed bar are equivalent to those of a plain round bar having the same weight per foot as the deformed bar.

b. Bar numbers are based on the number of eights of an inch included in the nominal diameter of the bars.

TABLE 7. STANDARD UNITED STATES REINFORCING BARS;
FULL SCALE, 1/60 SCALE, AND 1/90 SCALE

STANDARD U.S. REINFORCING BAR			SCALED DIMENSIONS			
			SCALE = 1/60		SCALE = 1/90	
BAR NO.	DIAMETER (in)	AREA (in ²)	DIAMETER (in)	AREA (in ² x10 ⁻⁴)	DIAMETER (in)	AREA (in ² x10 ⁻⁴)
2	0.250	0.05	.0042	.1364	.0028	.061
3	0.375	0.11	.0062	.302	.0042	.136
4	0.500	0.20	.0083	.545	.0056	.242
5	0.625	0.31	.0104	.852	.0069	.379
6	0.750	0.44	.0125	1.227	.0083	.545
7	0.875	0.60	.0146	1.670	.0097	.742
8	1.000	0.79	.0167	2.182	.0111	.970
9	1.128	1.00	.0188	2.776	.0125	1.234
10	1.270	1.27	.0212	3.519	.0141	1.564
11	1.410	1.56	.0235	4.337	.0157	1.938
14S	1.693	2.25	.0282	6.253	.0188	2.779
18S	2.257	4.00	.0376	11.110	.0251	4.940

leveled and sighted on the target line. Loads were applied at approximately one pound increments. At each increment, after the deformation due to the loading stabilized, the targetline was again sighted and the change in length measured. A sketch depicting the test is shown in Figure 11.

The trick to successful tensile testing of wire is to develop good connections for the ends so that the wire ultimately breaks between the connections, not at a connection. The connections serve as the link between the upper support and wire, and wire and loading pail. The best connection was made up of two 3 x 1 1/2 x 1/8 inch plates held together by two bolts (Figure 12). The wire was inserted one to two inches between the plates which were then clamped together by tightening the bolts. Of utmost importance was that the wire be inserted straight between the plates, so that equal pressure was distributed over the wire's cross-section. Using the deformer, slight deformations were etched into the wire in order to decrease the cross-sectional area just enough to cause stress concentration at the deformation points. This served to divert breakage away from the connections. Still occasional tests resulted in failure at the connections. These tests were considered invalid and were not recorded.

The overall length of the wire was measured and recorded after 75 percent of the ultimate load was applied. At this point, straightness of the wire was insured. Generally, seven to nine inch lengths were tested.

The initial tensile tests were performed by simply loading to failure, but the resulting stress-strain curves were characterized by

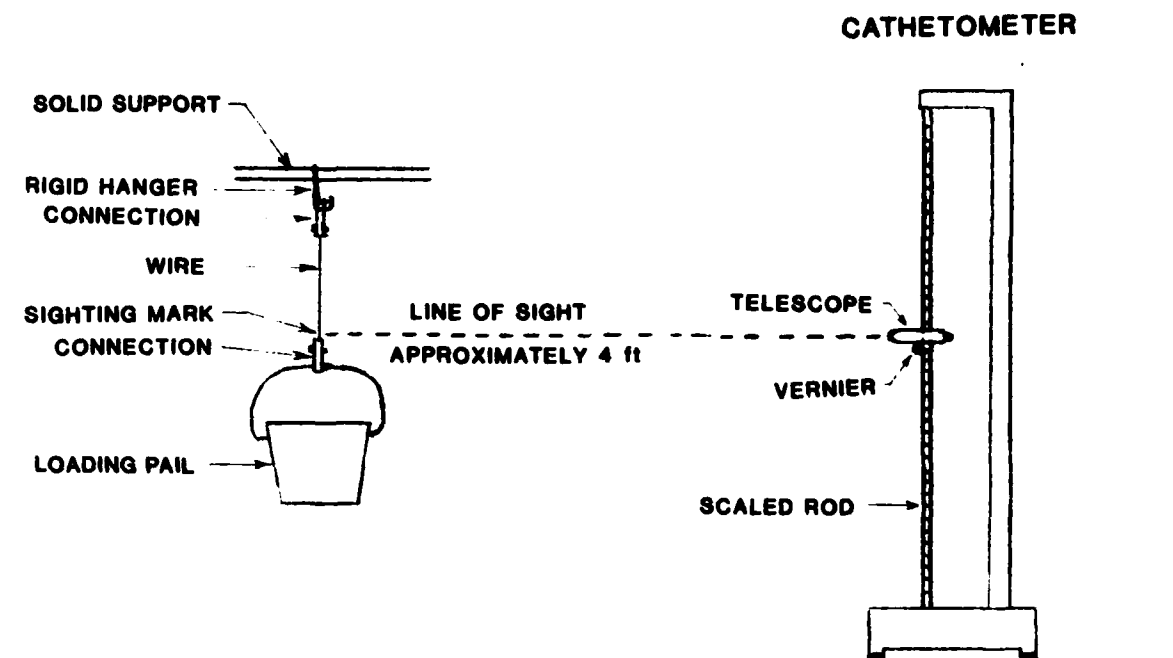


FIGURE 11. SCHEMATIC: TENSILE TEST OF REINFORCEMENT MATERIAL

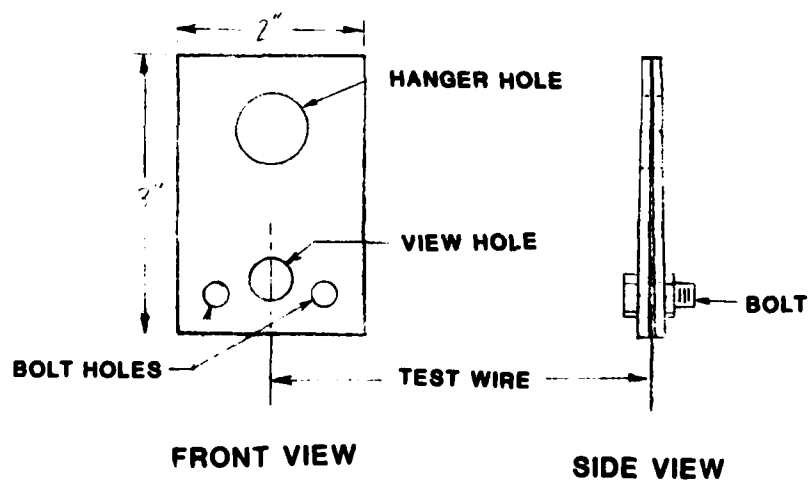


FIGURE 12. DETAIL CONNECTION

sporadic, large increases in strain and much lower than expected moduli of elasticities. It was surmised that some curvature and bending due to packaging and handling might exist in the wire, and that initial deformations might be due to straightening as well as elastic deformation.

Preloading the wire to a stress near the yield point solved the problem. Figure 13 is the plot of tensile stress versus strain. The first portion of the curve, data points represented by triangles, is the result of initial loading. Initial loading was terminated at a stress of 45,000 psi. At this stress the deformation is just entering the plastic zone.

The second portion of the curve, represented by astericks, is the result of incremental unloading. As expected, the slope of the unload curve is much greater and more consistent than the slope of the preload curve. This is because deformation due to unloading is strictly elastic since all sinuosity is removed by the initial load.

The final portion of the curve, represented by circles, shows the path of the stress versus strain curve as the wire is reloaded to failure. As shown, the reload curve follows the path of the unload curve, exhibiting a modulus of elasticity of 29,000,000 psi, which corresponds to that for the prototype reinforcement.

The wire could not be unloaded to zero stress due to the load imposed by the connection and weight hanger. The dashed line (Figure 13) is a projection of the unload and reload curves. The intersection of the dashed line and the abscissa defines the strain corresponding to zero stress. The yield point, defined as the stress at the point intersected by a line drawn at 0.2 percent offset from that strain, with

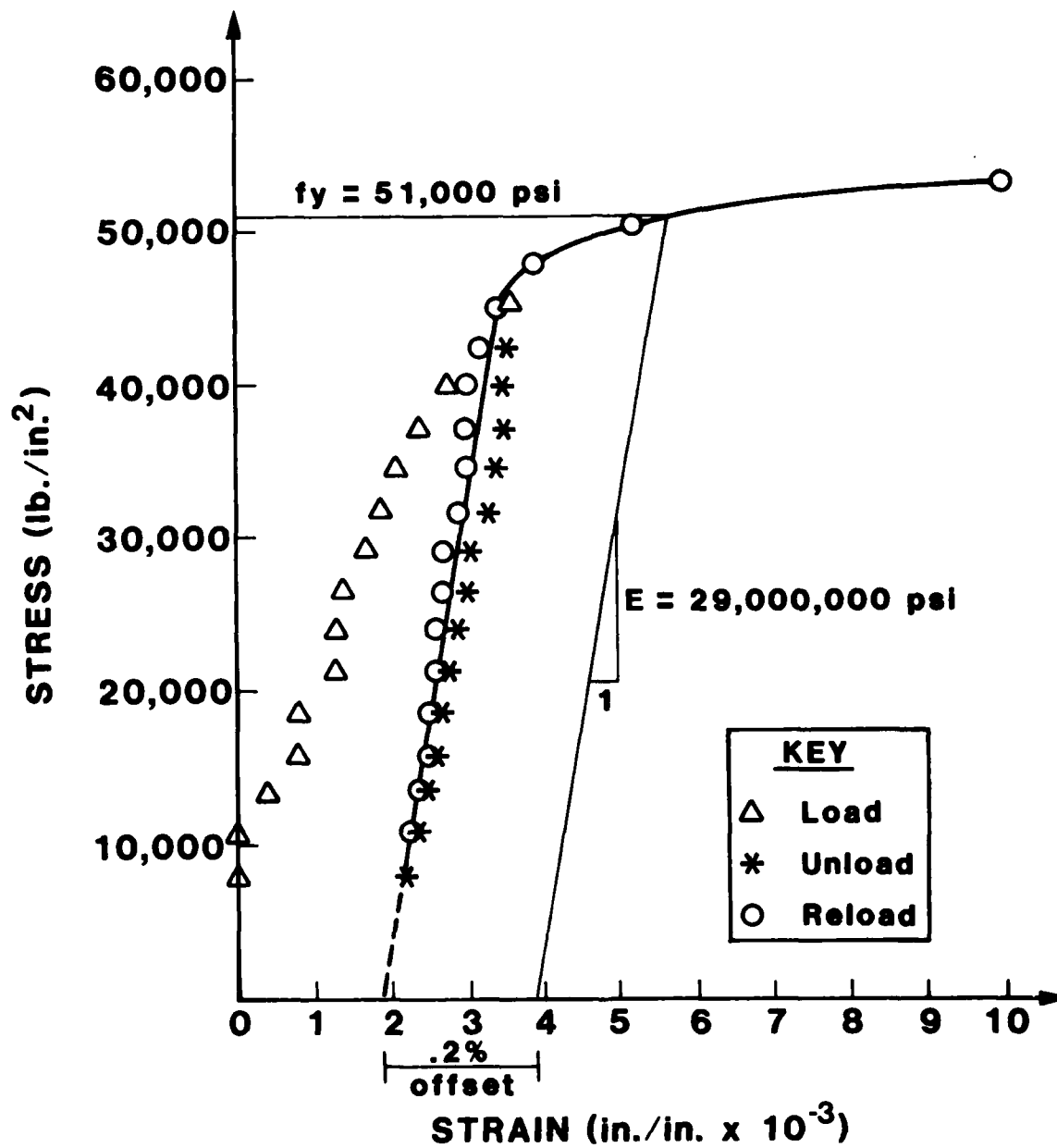


FIGURE 13. STRESS-STRAIN RELATION FOR TENSILE TESTING OF MODEL REINFORCEMENT

a slope equivalent to the modulus of elasticity, and the path of the stress versus strain curve, is 51,000 psi.

A total of 24 tensile tests were performed with excellent duplication of results. The wire tested was found to vary less than \pm three percent in diameter. However, it is recommended that the diameter of the wire being used as miniaturized reinforcement be checked periodically and that tensile tests be performed in conjunction with model testing.

The bond development between the miniaturized reinforcement and the microconcrete was insured by inwardly deforming the bars following the technique developed at Cornell. A deforming machine, made up of two pairs of perpendicularly mounted knurling wheels, was built. Features of the machine include: 1) pin mounted easy to change knurling wheels and 2) adjustable clearances between the two knurling wheels in each pair. The wire was hand pulled through the machine.

Several deformation-dimension ratios for prototype reinforcing bars are shown in Table 6. Based on the ratio of deformation to bar diameter, the spacing of the deformations on the miniaturized reinforcement was targeted for 70 percent of the diameter. The actual value was subject to available knurl size. The minimum depth of the deformation on the miniaturized reinforcement was set at five percent of the diameter. This dimension was based on the ratio of the minimum heights of the deformations to the diameter of the prototype bars.

Table 8 lists the miniaturized reinforcement by bar number (gauge size) and its corresponding weights, dimensions, and deformation specifications. The last column lists the knurling wheel used to deform each bar.

TABLE 8. MINIATURIZED REINFORCEMENT: WEIGHTS, DIMENSIONS, AND DEFORMATION SPECIFICATIONS

BAR NO.	WEIGHT (lb/ft)	DIA. (in)	AREA (in ²)	PERI. (in)	MAX* SPAC. (in)	MIN** HT. OF DEF. (in)	KNURL SPAC. (in)	HEIGHT OF DEF. USED (in)	ACTUAL HT. DIA. (in)	ACTUAL SPACING OF DEF. (in)	ACTUAL SPACING DIA. (in)	KNURL TEETH (in)
28	6.5×10^{-4}	.0162	2.0612×10^{-4}	.0509	.01134	.00081	.014	.0011	.0679	.0125	.77	80
24	14.1×10^{-4}	.0230	4.1548×10^{-4}	.0722	.0161	.00115	.020	.0015	.0652	.0125	.54	80
22	20.9×10^{-4}	.0286	6.4242×10^{-4}	.0898	.0200	.00143	.025	.0018	.0629	.0200	.7	50

* Based on Max spacing = .7(Dia)

Requirements of ASTM: A615-82

** Based on $\frac{\text{Min. Ht.}}{\text{Diameter}} = .05$

Key

PERI = Perimeter
 SPAC = Spacing
 HT = Height
 DEF = Deformation
 DIA = Diameter

SECTION VI

MICROCONCRETE-MINIATURIZED REINFORCEMENT INTERACTION

After designing the microconcrete and miniaturized reinforcement modelling materials, the suitability of the interaction of the materials was determined. To do this, a simple miniaturized reinforced concrete structure was built and subjected to loading. The load-deflection results were compared with the predicted results generated by the Non-linear Structural Analysis Program (NONSAPC) and, additionally, those predicted for a similar prototype using flexural strength computations.

The structure chosen was a simply supported beam with one row of steel placed in the tension zone. The beam was subjected to third point loading in order to develop a pure bending zone. The length and height of the beam, 7.3 inches and one inch respectively, correspond to the dimensions of the 1/60 scale model of the burster slab for the single bay model (7.3 x 7.3 x 1 inch). The width of the beam, .645 inches, was set to achieve a desirable height to width ratio of approximately 1.5.

The quantity of reinforcement placed in the beam was determined by the amount necessary to insure ductility. The range in which ductility is insured is defined by a minimum value determined by Equation 10.3 of the ACI code, and a maximum value determined by Equation 10.2.7 of the same (Reference 5).

The beam, including its dimensions, and location and quantity of reinforcement is shown in Figure 14. Also shown are the locations of the applied load and the supports.

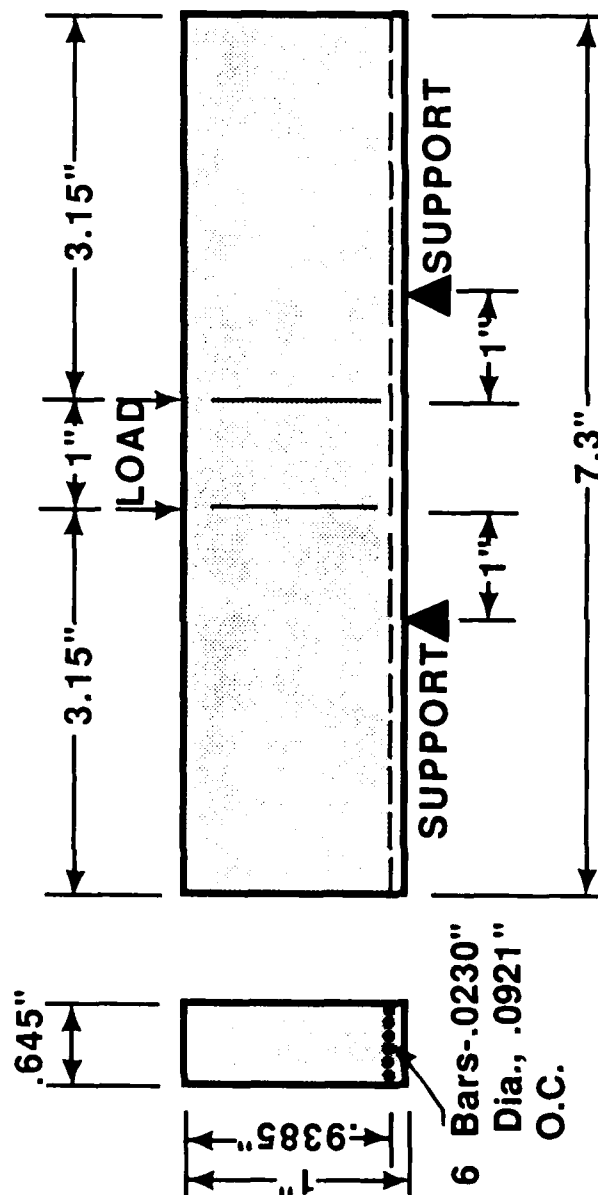


Figure 14. Schematic of Beam, and Location of Loading and Supports used in Beam Tests

To perform the beam test, special loading and support blocks were fabricated so that knife-edged contacts were made at the supports and at the location of the applied load. The load was applied using a compression converter adapted to the Department's Vishay Instruments BT-1000 testing machine. Displacement of the centerpoint at the bottom of the beam was measured using the Cathetometer. Load was applied slowly and displacements were measured at approximately 25 pound increments.

The results of two such tests are plotted in Figure 15. In these two tests fracture occurred through the center of the beam, insuring that the displacements measured were indeed, the maximum deflections. Also, no local crushing was observed at the contact points of load application or support. Local crushing at the knife edges, which occurred during several other tests, adversely affects the accuracy of the results.

The plots of the data show some discontinuity between points. However, the data, interpreted as a whole using a best fit curve, accurately represents the overall results of the beam load test. Individual readings were susceptible to slight inaccuracies due to insufficiencies of both equipment and the operator in dealing with measurements of such small magnitude. Total vertical displacement was approximately .006 inches. The Cathetometer accuracy was limited to .0004 inches by its graduation, or seven percent of the total displacement. Obviously, human error in the Cathetometer's telescope adjustments between readings is inherent to experimentation at this scale.

The results of the NONSAPC analysis (performed by Doug Yovaish) are also shown in Figure 15. This analysis was based on a beam of similar

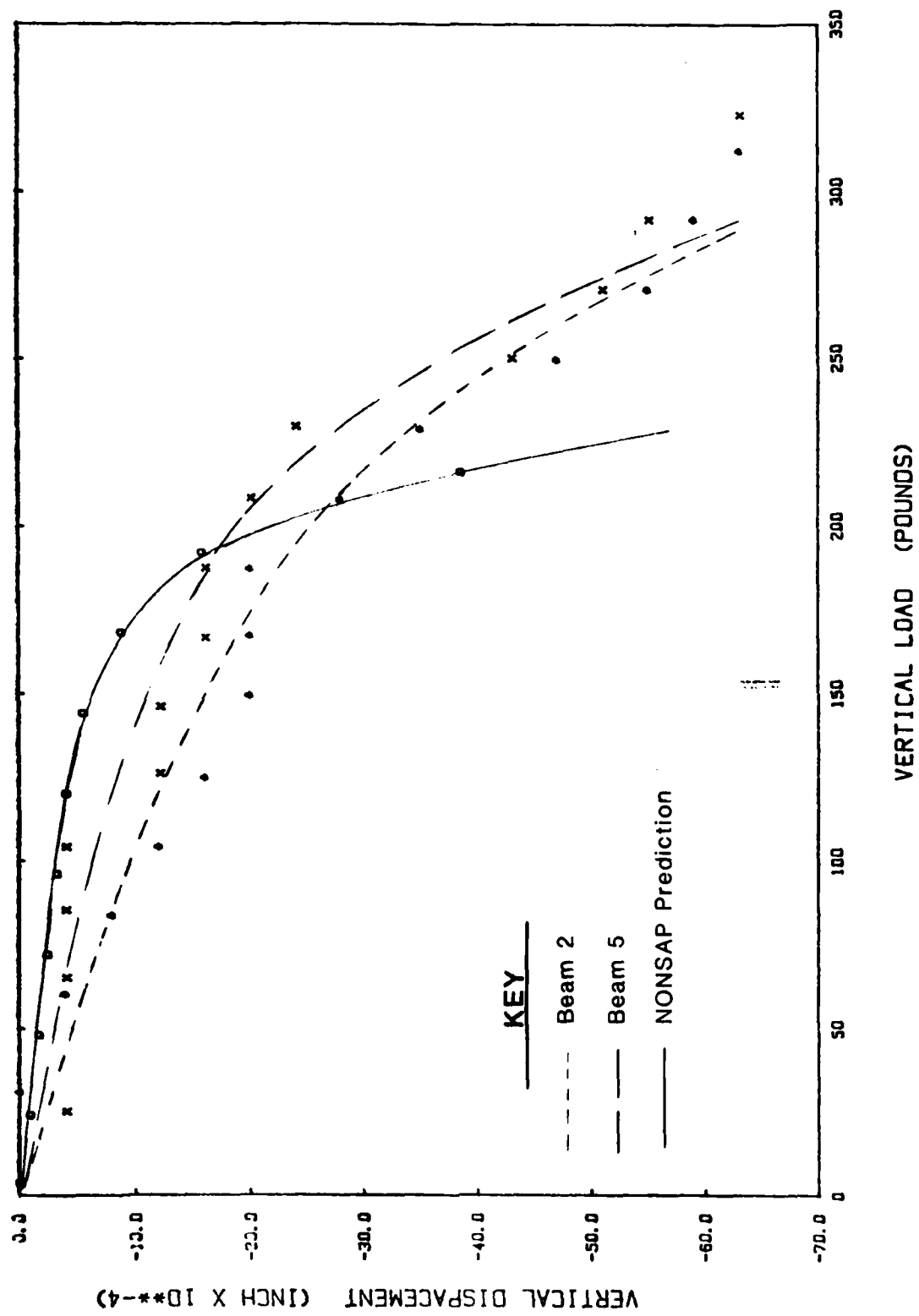


FIGURE 15. REINFORCED BEAM TESTS AND NONSAP PREDICTION

dimensions and loading conditions as the microconcrete test beam. The following parameters were used as input for into the program:

$$E_c = 3.3 \times 10^6 \text{ psi}$$

$$E_{st} = 29 \times 10^6 \text{ psi}$$

$$f'_c = 4000 \text{ psi}$$

$$f'_y (\text{steel}) = 51,000 \text{ psi}$$

$$\text{Composite } \nu = .3$$

$$\text{Coeff. of thermal expansion} = 6 \times 10^{-6} \text{ in/in/}^\circ\text{F}$$

Only the portion of the beam to the left of the centerline (see Figure 16) was modelled since the beam and loading were symmetric about the centerline.

The beam was divided into elements as shown on the second page of Figure 16. Seventy-two nodes were generated giving the model 192 degree of freedom. Nodes having restrained displacements are depicted by roller and pin connections in the figure. The load (1/4 of the vertical load plotted on the abscissa of Figure 15) was applied at two nodes, numbers 17 and 63. The reinforcement is modelled as a single bar of equal cross-sectional area. Vertical displacement was measured as the amount of downward movement at either node 28 or 64.

Good correlation exists between the actual tests and the NONSAPC model. The difference between the actual beam and the computer model is that the actual beam has an infinite number of degrees of freedom, while the computer model has 192.

The expected failure load, P , was computed using flexural strength analysis as suggested by Wang and Salmon (Reference 15). The load is determined from the following three equations:

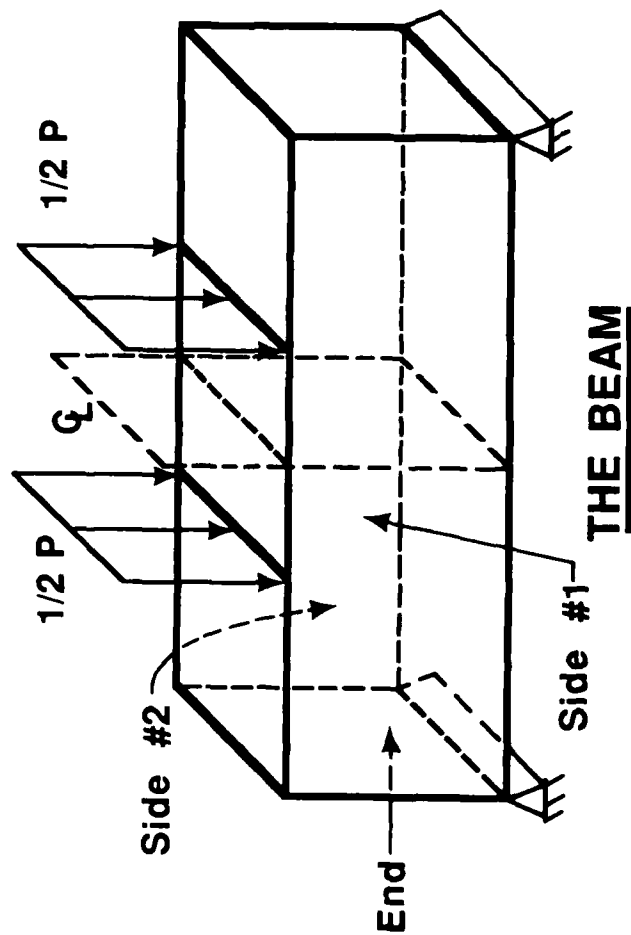


Figure 16. Nonsapc Model

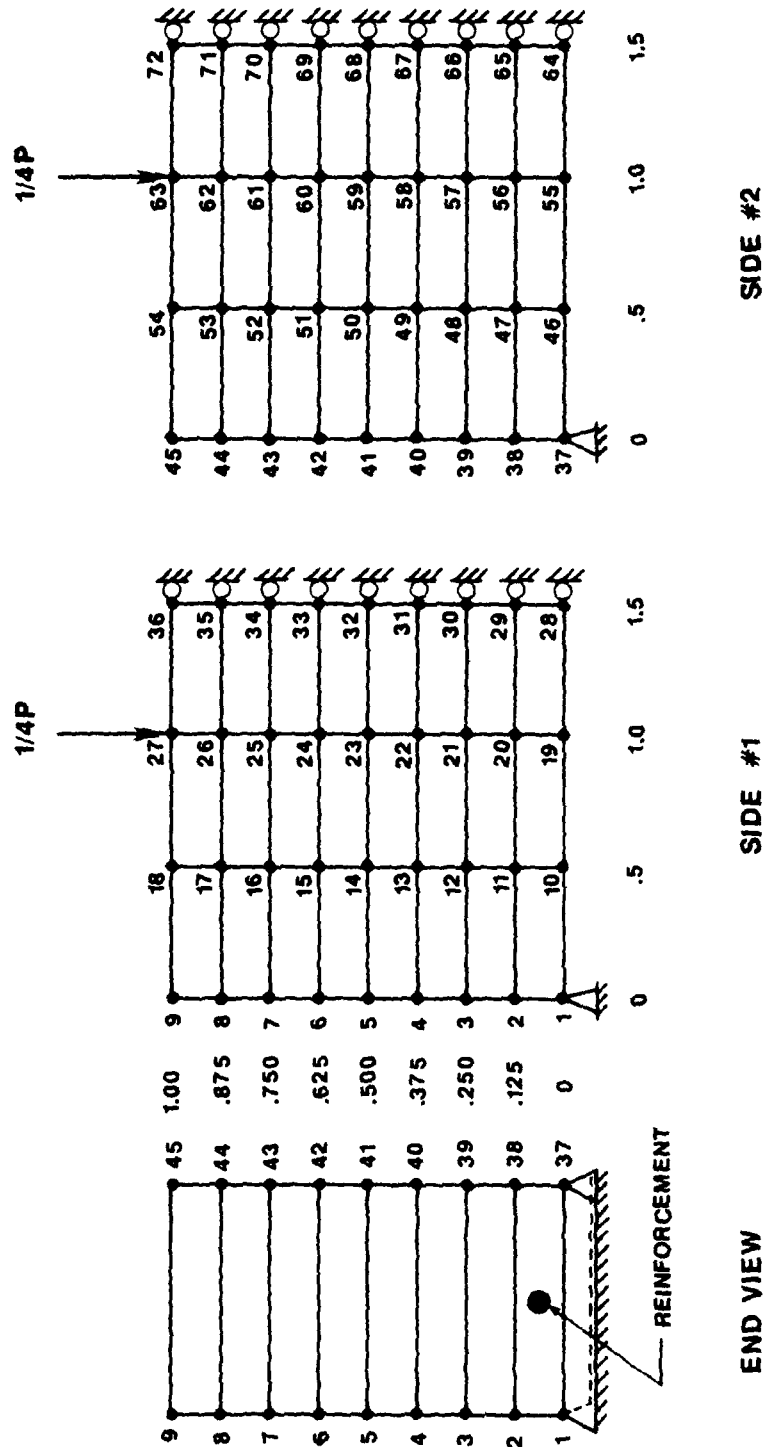


FIGURE 16 cont. ELEMENTS, NODES, NODE NUMBERS, AND POSITIONS OF LIMITED FREEDOM
(SCALE: 1" = 0.5")

$$1) \ a = \frac{A_s f_y}{.85 f'_c b}$$

$$2) \ M_n = A_s f_y (d - \frac{a}{2})$$

$$3) \ P = \frac{6M}{L}$$

where, A_s = area of steel

f_y = yield strength of steel

f'_c = compressive strength of concrete

b = width of beam

M_n = nominal flexural strength based on ultimate strength

d = depth of beam

P = load

$$a = \frac{A_s f_y}{.85 f'_c b} = \frac{(2.49288 \times 10^{-3})(51,000 \text{ lb/in}^2)}{.85(4085 \text{ lb/in}^2)(.645 \text{ in})} = 5.677 \times 10^{-2} \text{ in.}$$

$$\begin{aligned} M_n &= A_s f_y (d - \frac{a}{2}) = (2.49288 \times 10^{-2} \text{ in}^2)(51,000 \text{ lb/in}^2)(1 - \frac{5.677 \times 10^{-2}}{2}) \text{ in} \\ &= 123.5 \text{ in-lb} \end{aligned}$$

$$P = \frac{6M_n}{L} = \frac{6(123.5 \text{ in-lb})}{3 \text{ in}} = \underline{\underline{247.0 \text{ lbs.}}}$$

The model beams consistently broke at loads just over 300 pounds. This value is sufficiently close to the predicted value. The error is of the same magnitude, and allegedly due to the same cause, as the error associated with the modulus of rupture of the microconcrete (see Section IV).

Several qualitative results are also gained from this phase of testing. The microconcrete was workable at the small volume, flowing

smoothly into the form when vibrated. Visual inspection of the beam's cross-section after breaking revealed no segregation of particles nor excessive air voids.

The miniaturized reinforcement, which spanned 7.3 inches between end supports, adequately retained its position of placement during casting. Bond was developed between the miniaturized reinforcement and the microconcrete. No excessive voids were noticed in this area, and in no test was reinforcement pullout the mode of failure.

Plexiglass proved to be an excellent formwork material. After twelve beams were poured, the forms were still functioning satisfactorily with no distortion in shape and no leakage of concrete at the joints.

SECTION VII

DEVELOPMENT OF STRUCTURAL MODELS

A. Background

In order to fit a model of the entire prototype structure into a two-foot diameter centrifuge bucket, it would have to be scaled down to 1/150 of its original size. However, it is not physically possible to build the model at such a small scale. For instance, the 2' 1 1/2" thick interior wall of the prototype structure would be reduced to .17 inch thick in the model, making the placement of the miniaturized reinforcement too difficult.

In order to construct models at a feasible working size, and to accommodate the size of the centrifuge bucket, components of the prototype structure should be modelled. The following models are recommended:

1. Single bay structure with burster slab at 1/90 scale,
2. Double bay structure with burster slab at 1/90 scale,
3. Single bay structure with burster slab at 1/60 scale.

B. Single Bay with Burster Slab - 1/90 Scale Model

The single bay model consists of a box structure and separate burster slab. The dimensions, except for length, are scaled from the prototype. To develop symmetry, both walls of the model are scaled from the exterior walls of the prototype. The length of the model is equal to its width in order to be consistent with the other two models. The

burster slab is of the same width and length dimensions as the roof slab of the bay.

The thickness of the burster slab is scaled directly from the prototype. The burster slab is cast separately from the box structure, since the two are separated in the prototype by a layer of soil.

C. Double Bay with Burster Slab - 1/90 Scale Model

The double bay model consists of a double box structure and a separate burster slab. The dimensions, except for length, are scaled from the prototype. The exterior walls of the model are scaled from the exterior walls of the prototype. Likewise, the interior wall of the model is scaled from one of the two identical interior walls of the prototype. The length of the model is equal to its width. This dimension was set based on geometry to maximize the size of the model to fit the circular centrifuge bucket.

The burster slab is of the same width and length dimensions as the roof slab. The thickness of the burster slab is scaled directly from the prototype. Again, the burster slab is cast separately from the box structure.

D. Single Bay with Burster Slab - 1/60 Scale Model

This model was designed to serve as a model of the 1/90 scale single bay model. The two models are identical except for the difference in size.

E. General

The prototype structure, excluding the burster slab, is heavily reinforced with steel. Figure 17 shows the locations of the major reinforcing bars in the floor slab, ceiling slab, exterior walls and

interior walls of the three-bay portion of the prototype. The burster slab, also shown in Figure 17, contains only temperature steel.

Three considerations were made in the steel design of the models:

1. The overall area of steel was modelled. The yield stress of the miniaturized reinforcement, 51,000 psi, was less than the yield stress of the prototype reinforcement, 60,000 psi. Therefore, the scale factor, $S_{\sigma_{ST}} = 1.17647$ was applied to the already geometrically reduced area of the miniaturized reinforcement.
2. The locations of the miniaturized reinforcing bars relative to the dimensions of the model were to be identical to the locations of the prototype reinforcing bars relative to the dimensions of the prototype.
3. The size of each miniaturized reinforcing bar (choice of 22-, 24-, or 28-gauge) was chosen to be as close as possible to the size determined from the geometric and stress scale factor reduction.

Table 9 of this section is a summary of the quantity of reinforcement of both the prototype and the model.

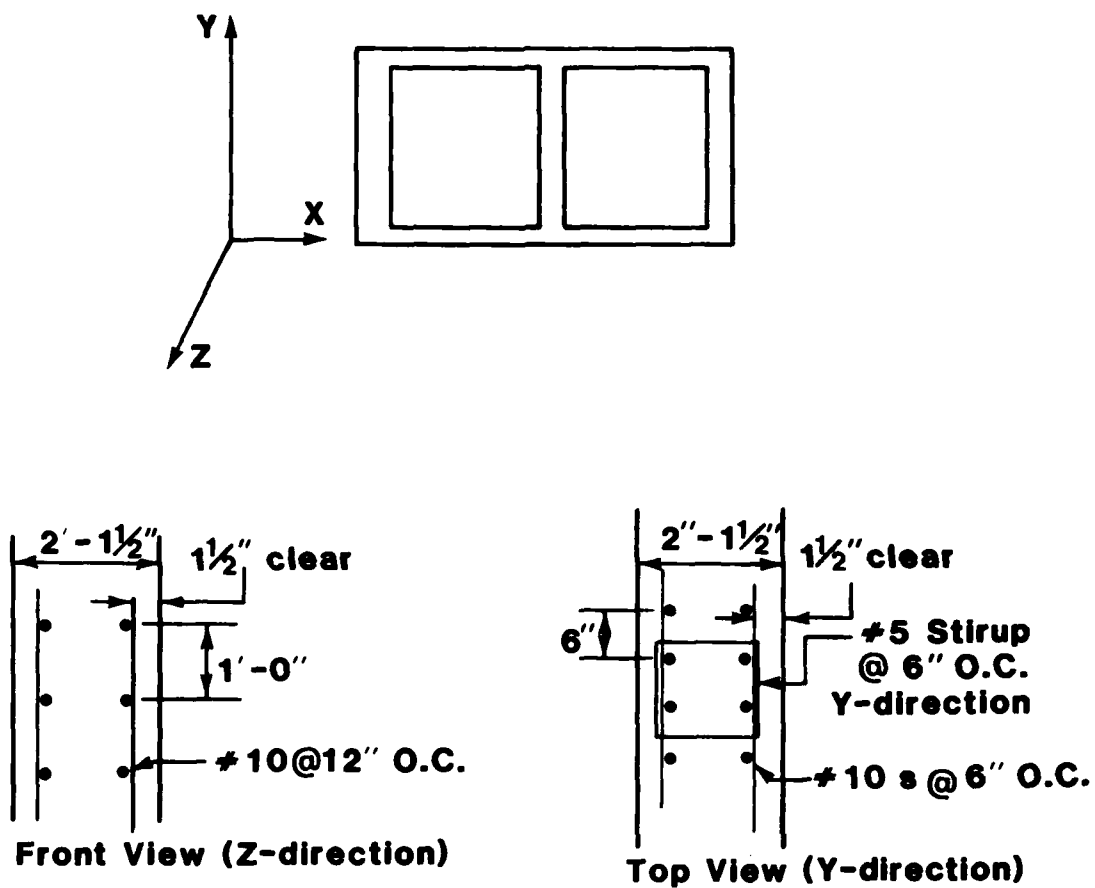
Detailed structural drawings for the proposed models are shown in the following figures:

Figure 18 - 1/90 Scale Single Bay

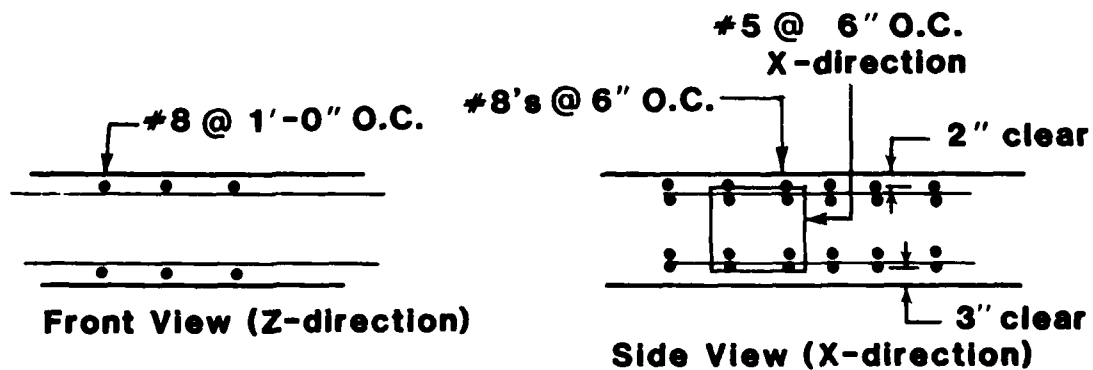
Figure 19 - 1/90 Scale Double Bay

Figure 20 - 1/60 Scale Single Bay

Detailed structural drawings of the corresponding burster slabs are shown in Figure 21.

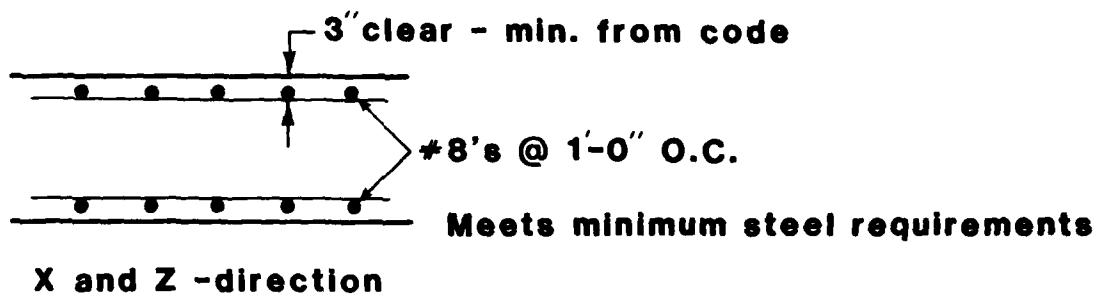


Steel Detail (Interior Wall)

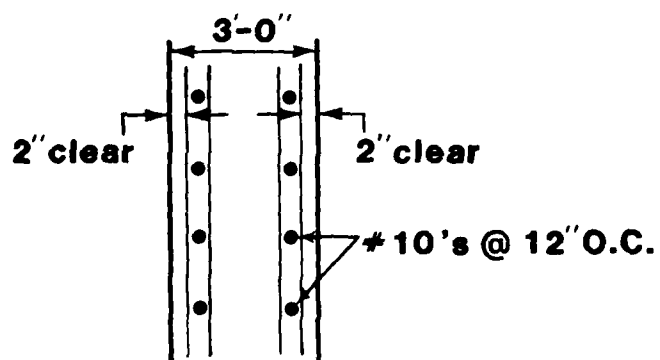


Steel Detail (Floor Slab)

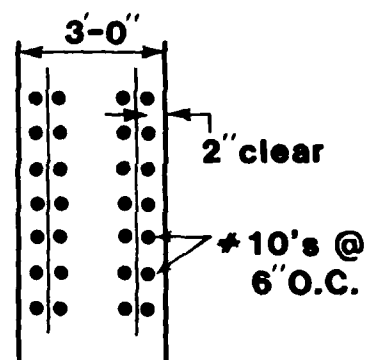
FIGURE 17. PROTOTYPE STRUCTURAL DETAILS



Steel Detail (Burster Slab)

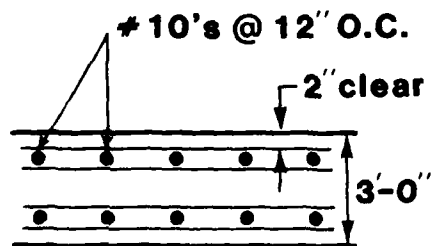


Front View (Z-direction)

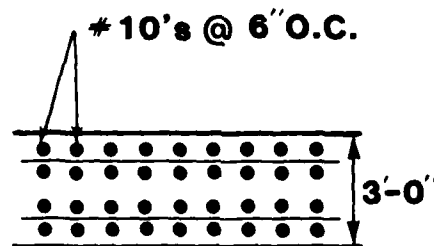


Top View (Y-direction)

Steel Detail (Exterior Wall)



Front View (Z-direction)



Side-View (X-direction)

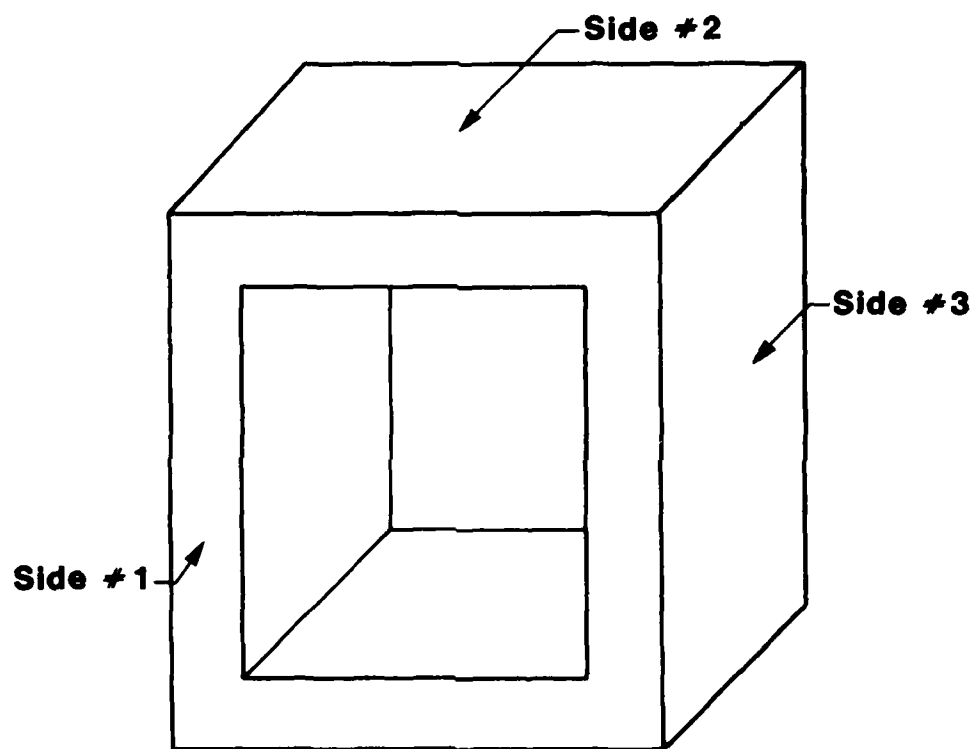
Steel Detail (Roof Slab)

FIGURE 17. (CONTINUED)

TABLE 9. SUMMARY OF STEEL REINFORCEMENT QUANTITIES

STRUCTURE	PROTOTYPE AREA OF REINFORCEMENT (in ²)	MODEL AREA OF REINFORCEMENT (in ²)	SIMILITUDE REQUIREMENT - AMOUNT USED SIMILITUDE REQUIREMENT x 100%
1/90 Scale Single Bay:			
Roof Slab	261.62	3.867×10^{-2}	1.96
Floor Slab	162.74	2.406×10^{-2}	-1.79
Exterior Wall	<u>264.16</u>	<u>3.908×10^{-2}</u>	<u>-1.86</u>
TOTAL	688.52	10.181×10^{-2}	-1.81
Burster Slab	33.18	4.819×10^{-3}	2.56
1/90 Scale Double Bay:			
Roof Slab	469.90	6.885×10^{-2}	-.88
Floor Slab	292.30	4.27×10^{-2}	-.64
Interior Wall	243.84	3.567×10^{-2}	-.71
Exterior Wall	<u>431.80</u>	<u>6.349×10^{-2}</u>	<u>-1.24</u>
TOTAL	1437.84	21.071×10^{-2}	-.90
Burster Slab	58.46	8.491×10^{-3}	1.94
1/60 Scale Single Bay:			
Roof Slab	261.62	8.550×10^{-2}	0.0
Floor Slab	162.74	5.320×10^{-2}	-.03
Exterior Wall	<u>264.16</u>	<u>8.633×10^{-2}</u>	<u>0.0</u>
TOTAL	688.52	22.503×10^{-2}	-.01
Burster Slab	33.18	1.084×10^{-2}	-.33

1/90 Single Bay Model



Scale - Full

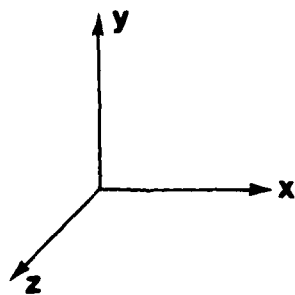
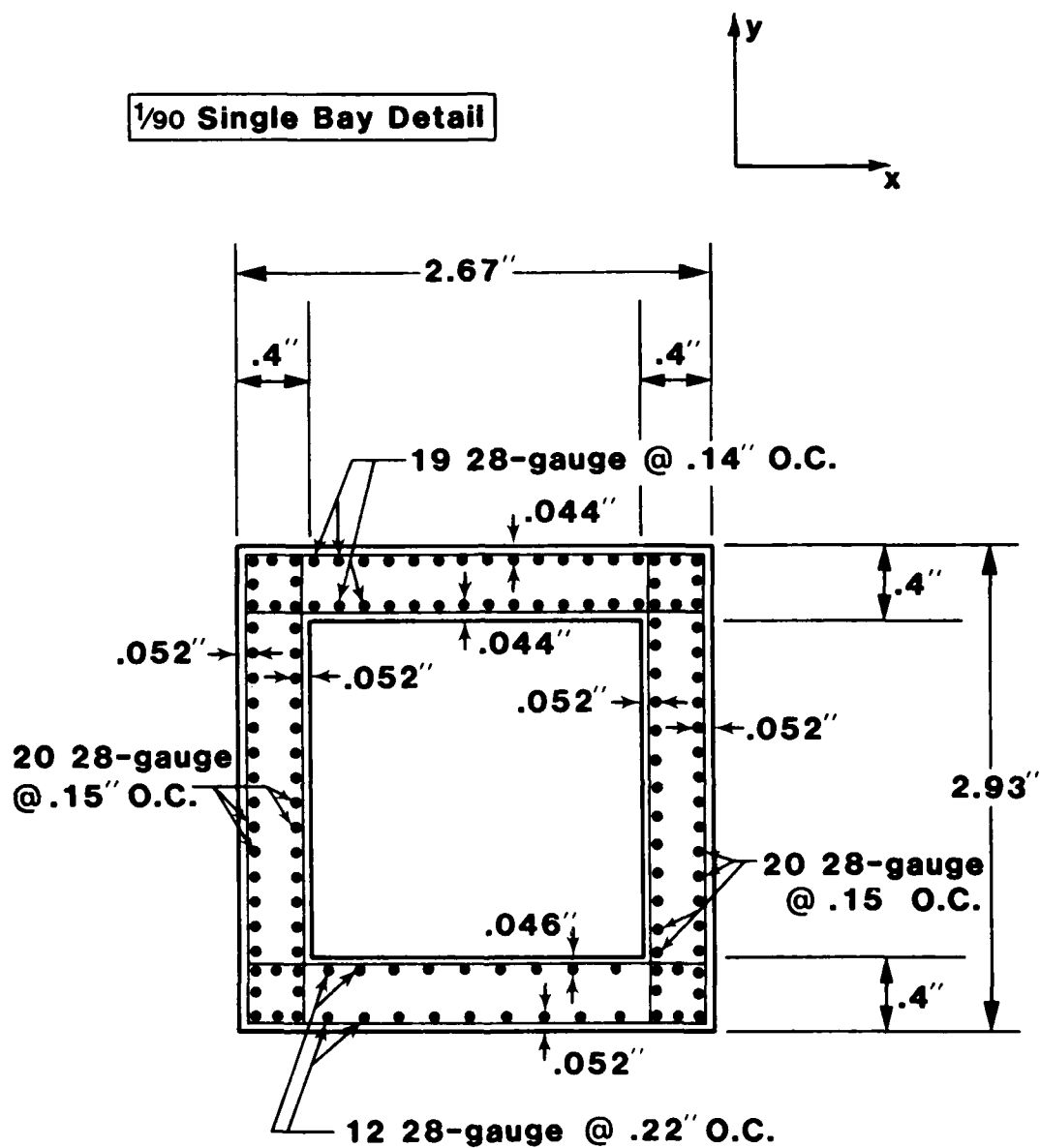


FIGURE 18. STRUCTURAL DETAILS - 1/90 SCALE SINGLE BAY MODEL

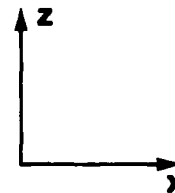


Detail - Side #1

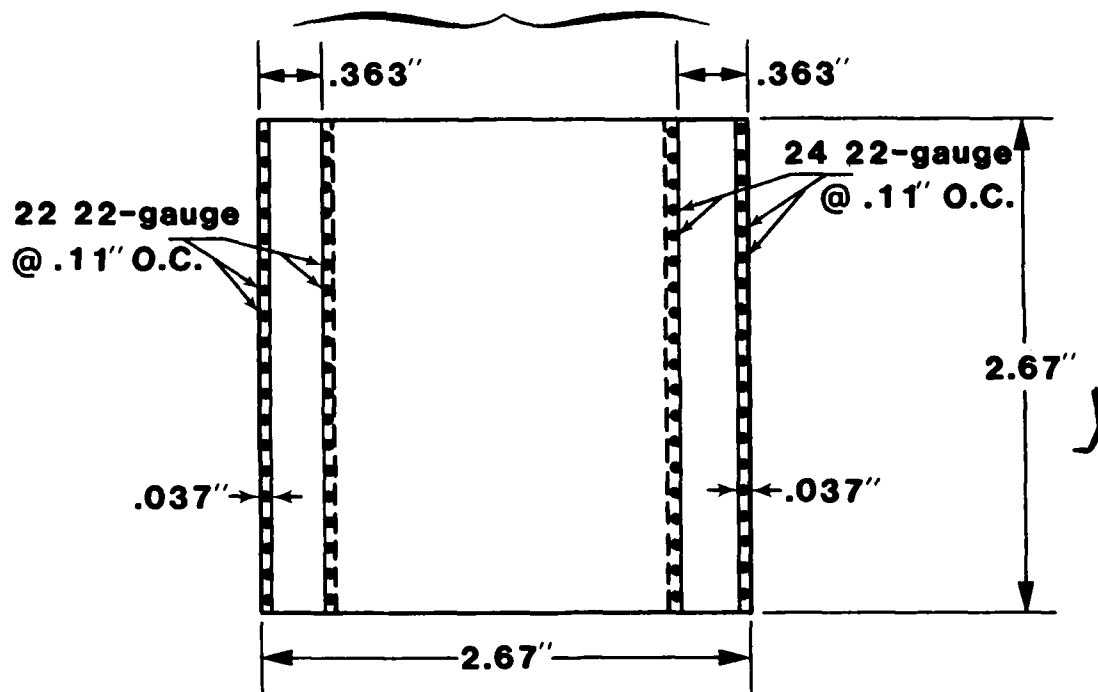
Scale - Full

FIGURE 18. (CONTINUED)

1/90 Single Bay Detail



Dimension indicates distance from edges to center of reinforcement in inside rows.

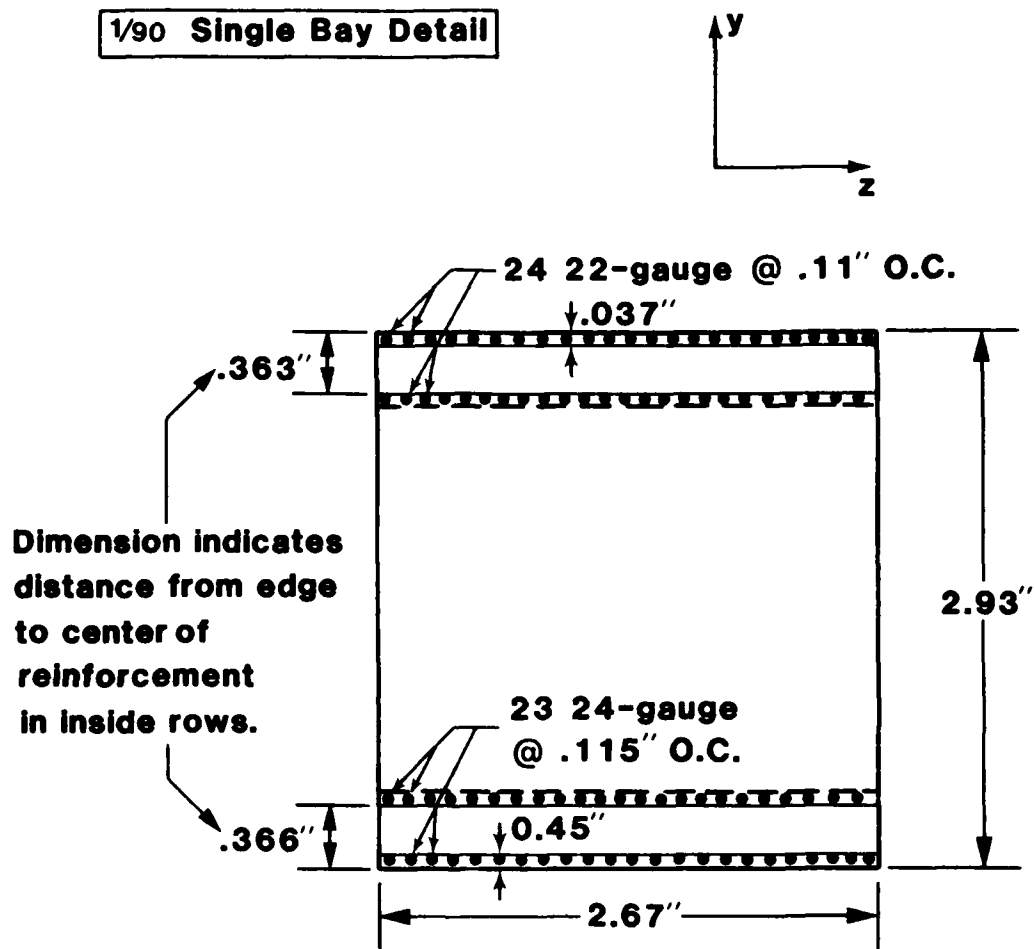


Detail - Side #2

Scale - Full

FIGURE 18. (CONTINUED)

1/90 Single Bay Detail



Detail - Side #3

Scale - Full

FIGURE 18. (CONTINUED)

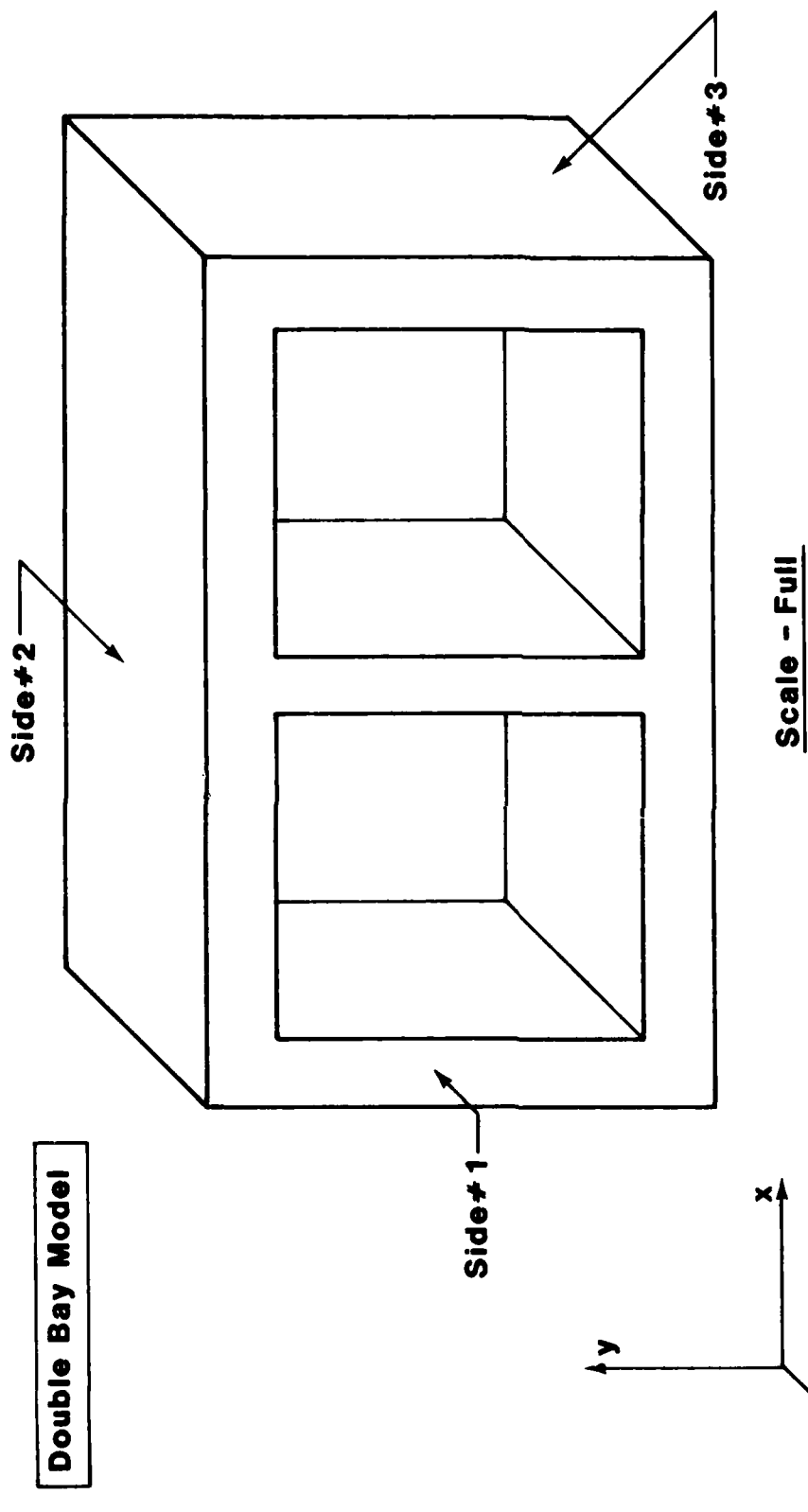
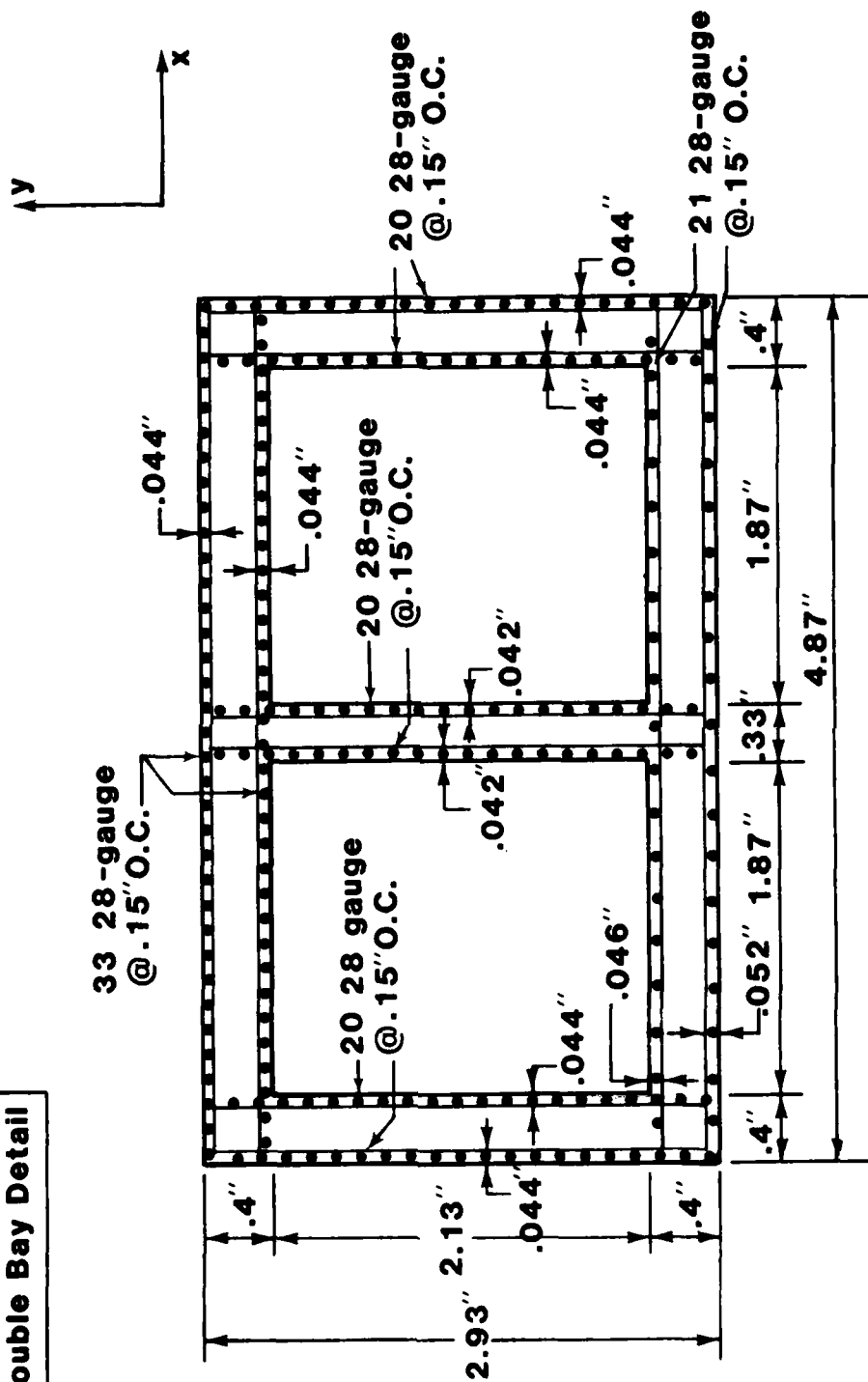


FIGURE 19. STRUCTURAL DETAILS - 1/90 SCALE DOUBLE BAY MODEL

Double Bay Detail



Detail - Side #1

Scale - Full

FIGURE 19. (CONTINUED)

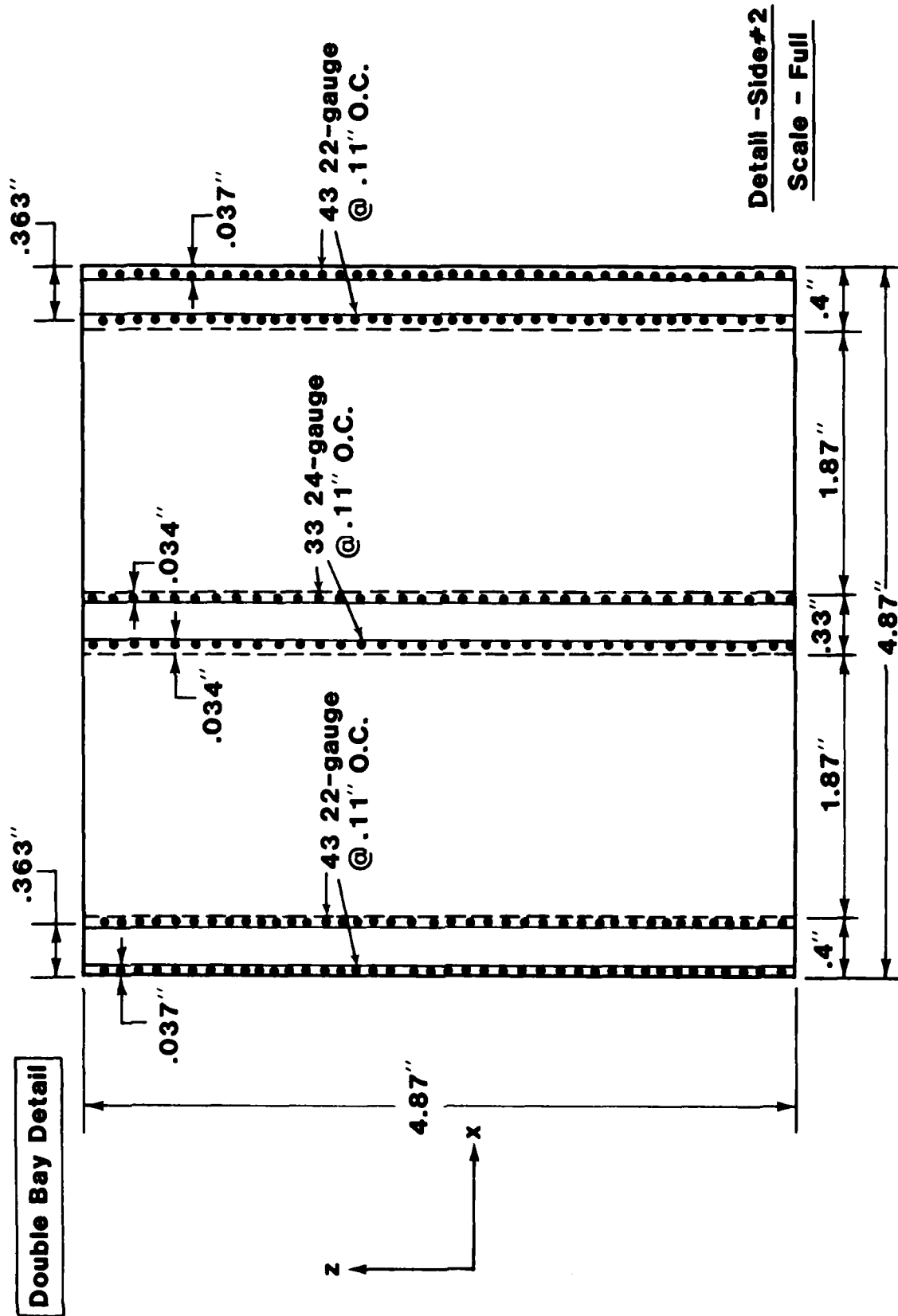
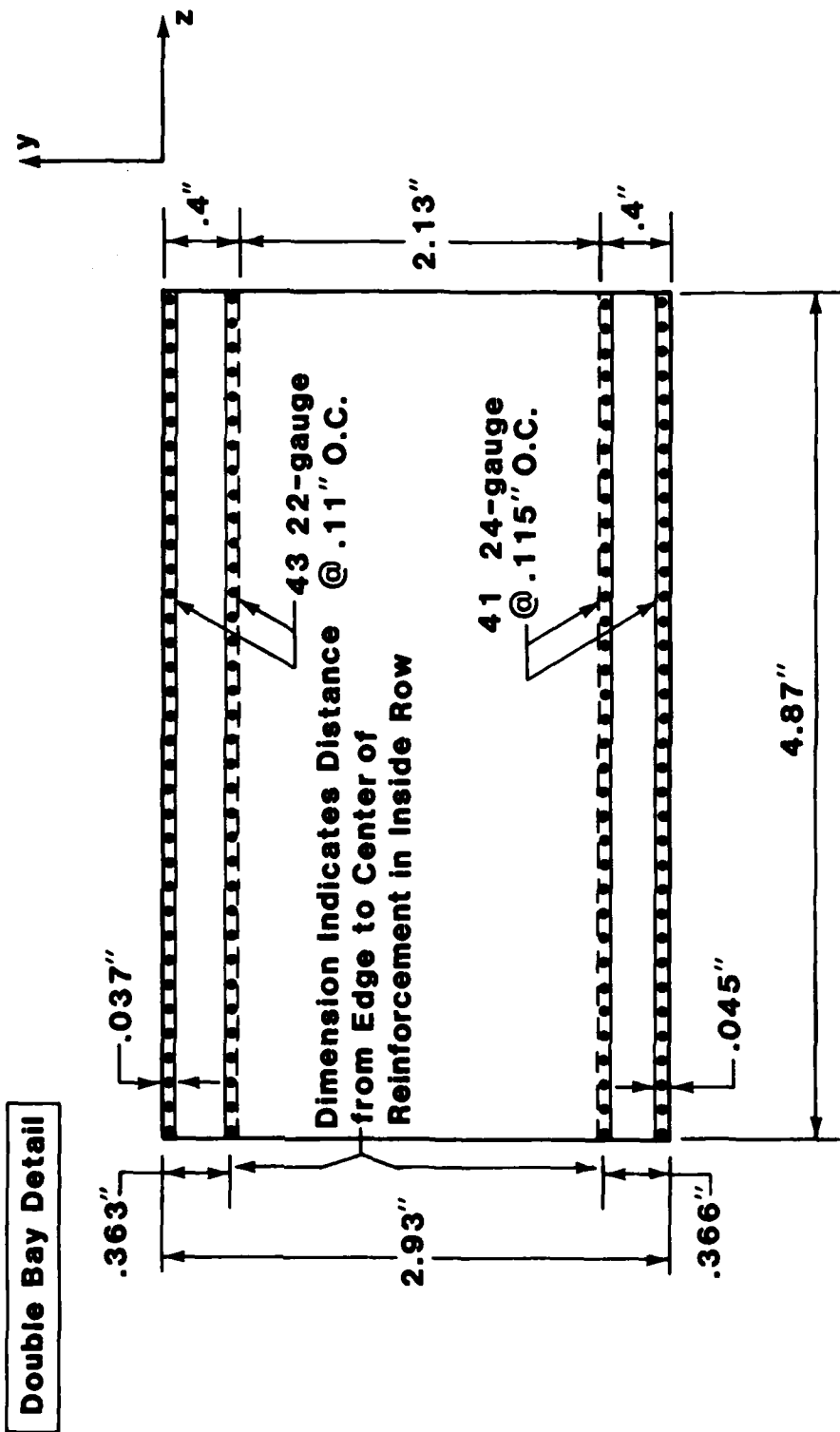


FIGURE 19. (CONTINUED)

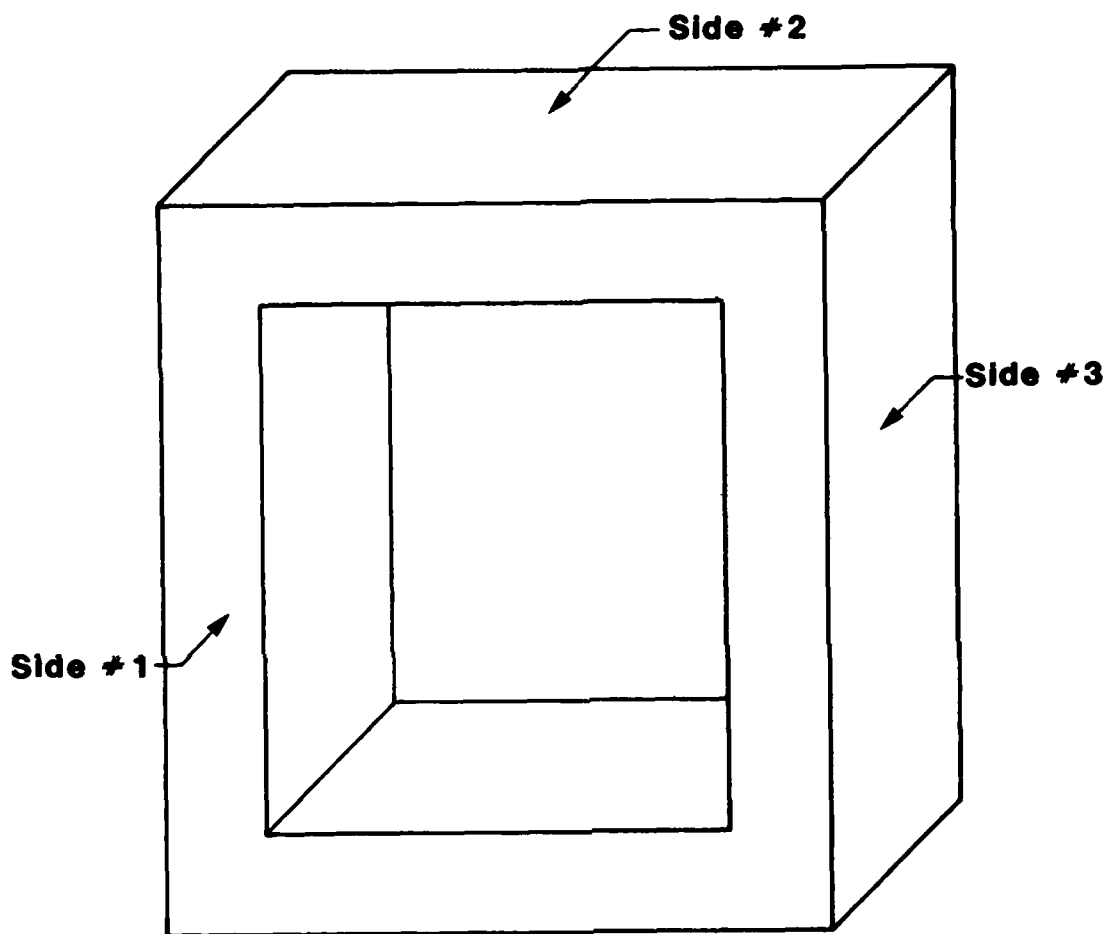


Detail - Side #3

Scale - Full

FIGURE 19. (CONTINUED)

1/60 Single Bay Model



Scale - Full

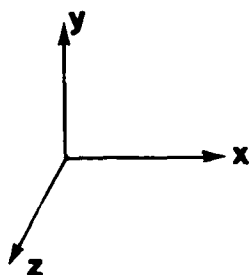


FIGURE 20. STRUCTURAL DETAILS - 1/60 SCALE SINGLE BAY MODEL

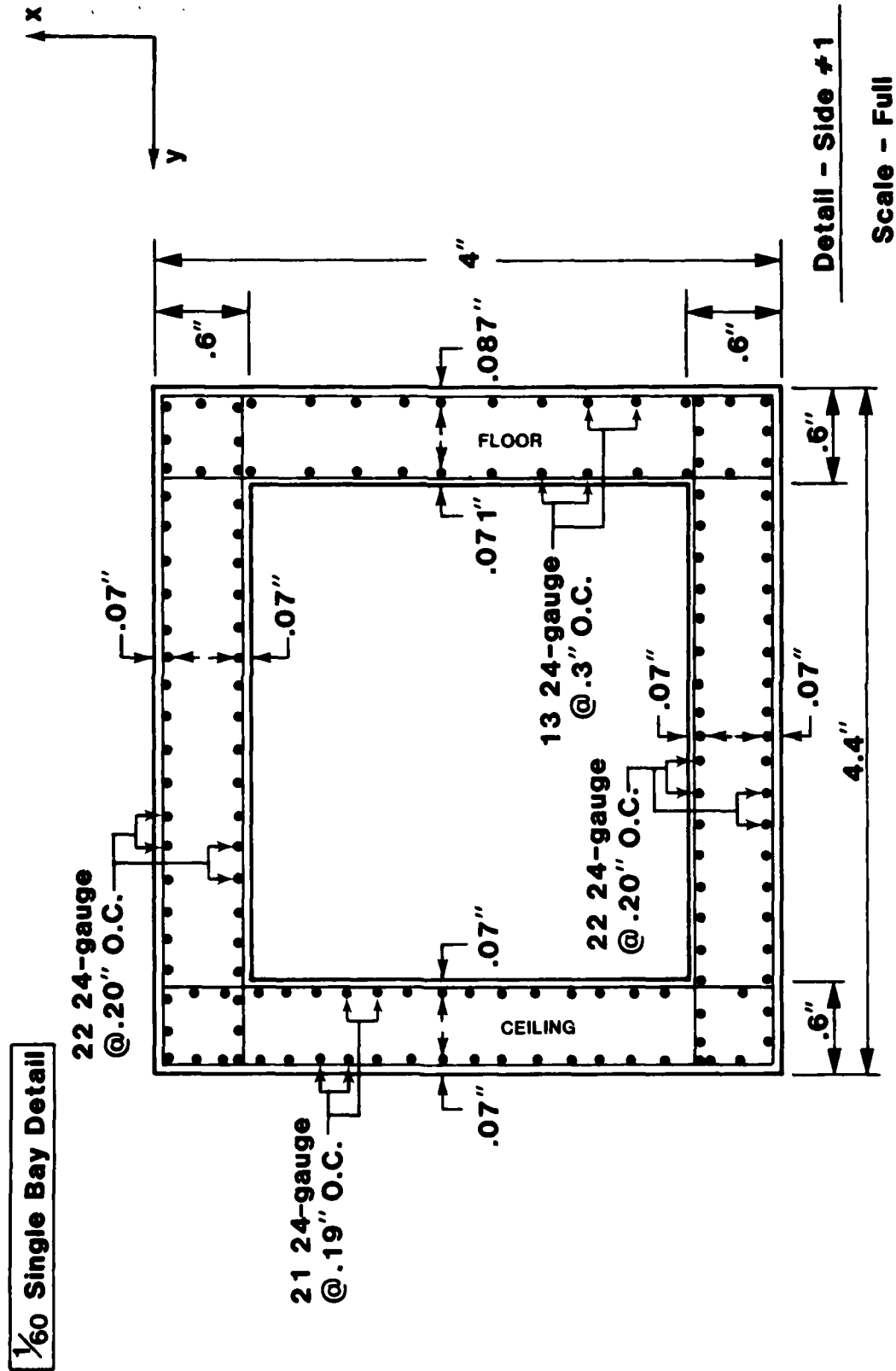
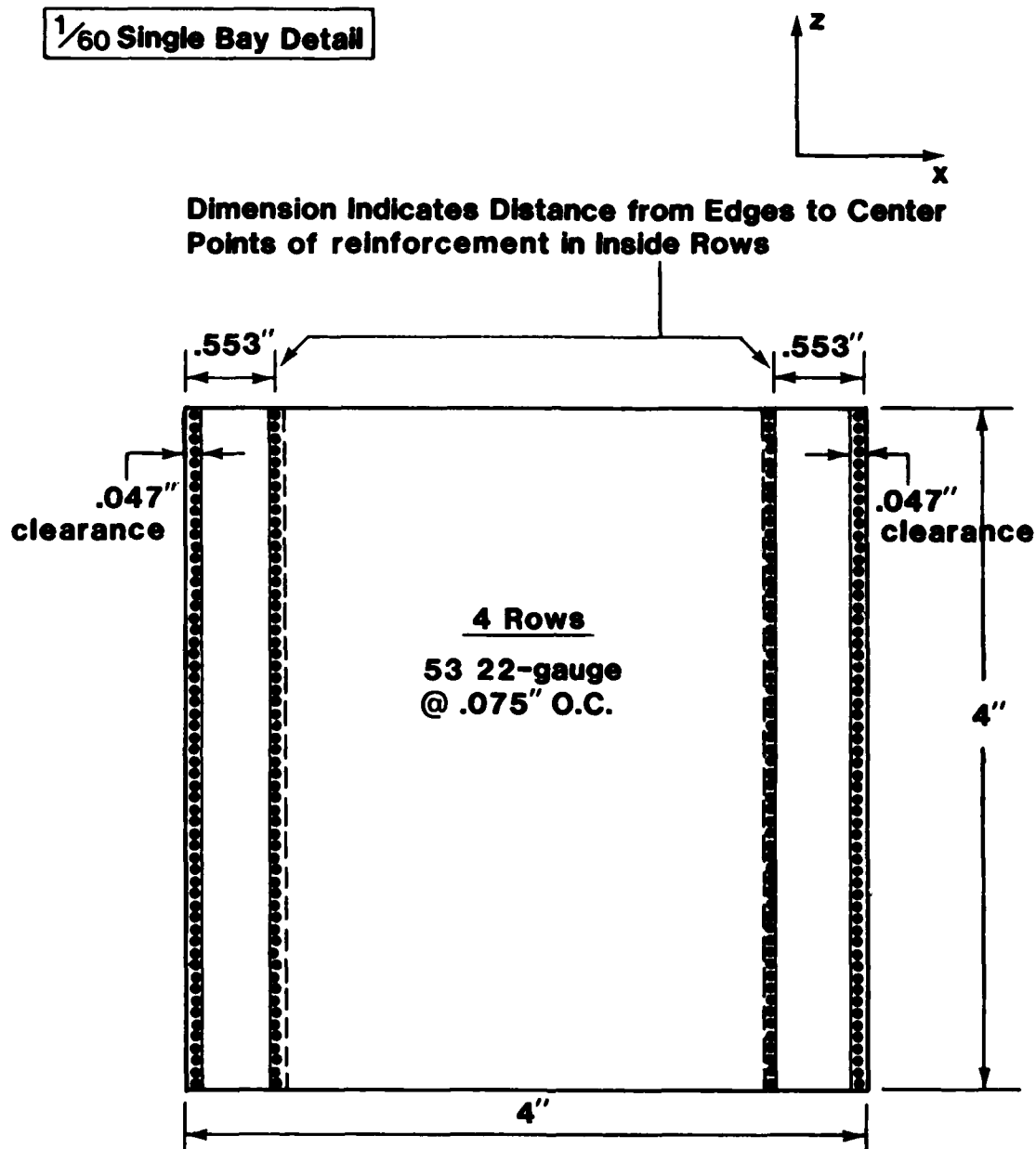


FIGURE 20. (CONTINUED)

1/60 Single Bay Detail

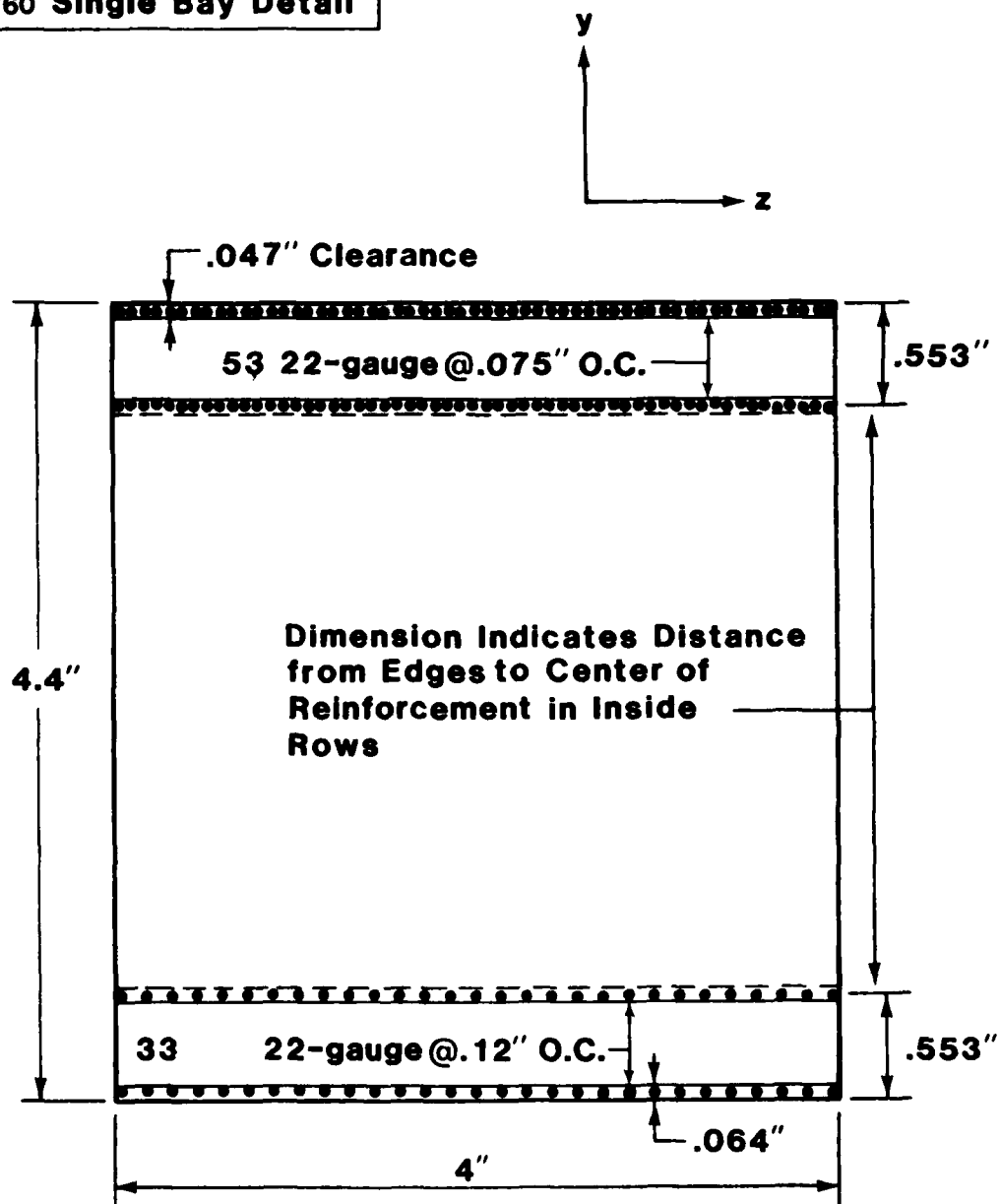


Detail - Side #2

Scale - Full

FIGURE 20. (CONTINUED)

1/60 Single Bay Detail

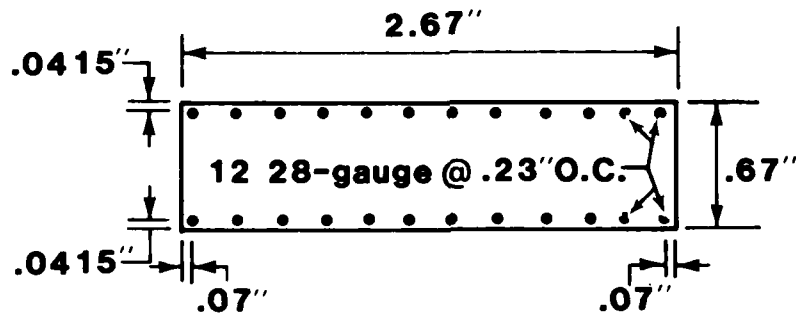


Detail - Side #3

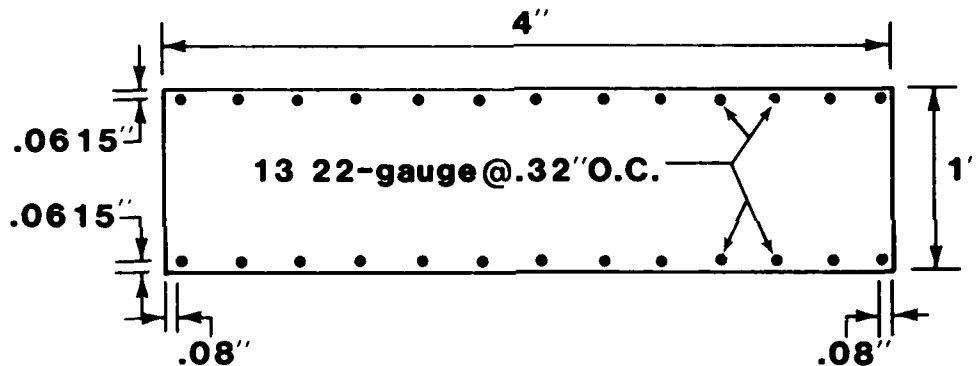
Scale-Full

FIGURE 20. (CONTINUED)

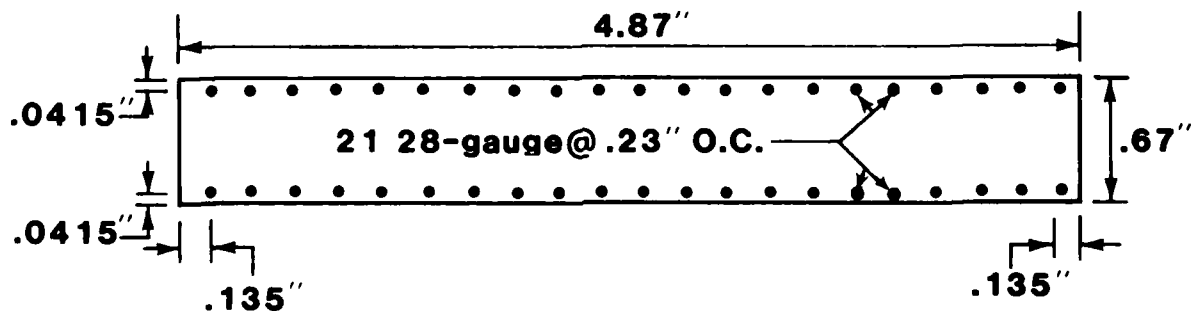
Detail - Burster Slab ($\frac{1}{90}$ Single Bay)



Detail - Burster Slab ($\frac{1}{60}$ Single Bay)



Detail - Burster Slab ($\frac{1}{90}$ Double Bay)



Scale - Full

FIGURE 21. STRUCTURAL DETAILS - BURSTER SLABS

SECTION VIII

CONCLUSION AND RECOMMENDATION

A. Conclusion

Following the modelling procedures established in this report, models of the entire prototype structure, or its components, will simulate the prototype in response to static, and hopefully dynamic, loading.

Additionally, based on the results of the reinforced beam test, the physical model's response to static loading approximates that predicted by the NONSAPC computer analysis.

The microconcrete and miniaturized reinforcement recommended in this report will develop the following scale factors in relation to the prototype structure, resulting in the development of a true model:

<u>QUANTITY</u>	<u>DIMENSION</u>	<u>SCALE FACTOR</u>
Concrete Stress	FL ⁻²	$S_{\sigma_c}=1$
Concrete Modulus	FL ⁻²	$S_{E_c}=1$
Reinforcement Stress	FL ⁻²	$S_{\sigma_r}=1.176$ (based on yield stress)
Reinforcement Modulus	FL ⁻²	$S_{E_r}=1$
Poisson's Ratio		$S_{\nu}=1$ (Assumed)
Density	FL ⁻³	$S_{\rho}=1$

The geometric scale factors follow:

<u>QUANTITY</u>	<u>SCALE FACTOR</u>
Linear Dimension	$S_L = n$
Area of Reinforcement	$S_{A_r} = n^2 S_{\sigma_r}$

where n = number of gravities induced by the centrifuge.

B. Recommendation

It is recommended that the three component models specified in this report be tested in a centrifugal environment, in conjunction with computer analyses. If the computer analyses successfully predict the centrifugal model events, then centrifugal modelling of the entire prototype structure may not be required.

REFERENCES

1. Murphy, G.; "Similitude in Engineering," Ronald Press Co., New York, New York, 1950.
2. Bradley, D.; Townsend, F.C.; Fagundo, F.E.; Davidson, J.L.; "Centrifugal Scaling Laws for Ground Launch Cruise Missile Shelter," Department of Civil Engineering, University of Florida, April, 1984.
3. Zia, P.; White, R.N.; and VanHorn, D.A.; "Principles of Model Analysis," ACI Publication No. 24, 1970.
4. Chawdbury, A.H.; White, R.N.; and Scott, N.R.; "Small Scale Models for Reinforced Concrete Structures," ASAF, Vol 20, 1977.
5. "Building Code Requirements For Reinforced Concrete (ACI 318-77)," American Concrete Institute, 4th Printing, March, 1979.
6. White, R.N.; Sahnis, G.M.; and Harris, H.G.; "Small Scale Direct Models of Reinforced and Prestressed Concrete Structures," Report No. 326, Department of Structural Engineering, School of Civil Engineering, Cornell University, Ithaca, New York, Sept., 1966.
7. Mirza, M.S.; "An Investigation of Combined Stresses in Reinforced Concrete Beams," Ph.D. Thesis, Structural Series No. 1, McGill University, Montreal, Canada, March 1967.
8. Sahnis, G.M.; and White, R.N.; "A Gypsum Mortar for Small-Scale Models," ACI Journal November, 1967.
9. Kandasamy, E.G.; "Stress-Strain Characteristics of Gypsum Plaster-Sand Mixes Under Direct and Flexural Compression," M.S. Thesis, North Carolina State University, Raleigh, 1969.
10. Mirza, M.S.; "Structural Concrete Models (Materials, Instrumentation, Correlation) A State-Of-The-Art Report," Department of Civil Engineering, McGill University, Montreal, Quebec, 1972.
11. Roll, F.; "Materials for Structural Models," Journal of the Structural Division, Proceedings of the American Society of Civil Engineers, June, 1968.
12. Harris, H.G.; Sahnis, G.M.; and White, R.N.; "Reinforcement for Small Scale Direct Models of Concrete Structures," ACI Publication No. 24, 1970.
13. Murayama, Y.; and Noda, S.; "Study on Small Scale Model Tests for Reinforced Concrete Structures--Small Scale Model Tests by Using 3mm Diameter Deformed Re-bars," Kajima Institute of Construction Technology, No. 19-1, February, 1983.

14. Southern California Chapter American Public Works Association and Southern California District Associated General Contractors of California Joint Cooperative Committee, "Standard Specifications for Public Works Construction," Building News, Inc., 1982.
15. Wang, C.K. and Salmon, C.G.; "Reinforced Concrete Design," Third Edition, Harper and Row, Publishers, Inc., 1979.

APPENDIX A

MODELLING MATERIALS AND PROCEDURES

A. MATERIALS

1. MICROCONCRETE
2. MINIATURE REINFORCEMENT
3. FORMWORK

B. MODEL CONSTRUCTION

C. PREPARATION OF TEST CYLINDERS

APPENDIX A
MODELLING MATERIALS AND PROCEDURES

A. MATERIALS

The three major components of a model are the microconcrete, the miniaturized reinforcement, and the formwork. The following is a description of the materials and procedures necessary for the preparation of each component, and procedures for the construction of the models. Included are notes which may be helpful in following the procedures.

The equipment specified is that used and recommended by the author. Equipment of equal capability may be substituted in future endeavors.

1. Microconcrete

Materials: Ultracal® 60
Edgar sand
Water

Equipment: Mixer (Heavy-duty, table-mounted, rotary type used by professional bakers)
#30, #50, #100, #200 mesh soil sieves and shaking machine
Drying oven
Electronic weight scale (Accuracy = 0.1 g)

Procedure:

- 1) Dry the Edgar sand in the drying oven.
- 2) Use soil sieves and the shaking machine to segregate the sand grains by particle size. Sieves with large surface areas are handy as large quantities of sand are needed. 18" x 30" sieves are capable of processing 10 pounds of sand at a time.
- 3) Keep the sand retained on the #50, #100, and #200 mesh sieves, leaving it segregated according to particle size. Discard the sand retained on the #30 mesh sieve.

- 4) Weigh the quantities of gypsum, sand, and water needed for the batch of microconcrete.

The ratio of gypsum(G):sand(S):water(W) is 1:.8:.25 by weight. The ratio of particle sizes of the sand as used as micro-aggregate is as follows:

<u>Sieve #</u>	<u>Percent sand by weight</u>
30	20
50	70
100	10
200	

The optimum size of one batch is 15 pounds total weight. This is enough mix to cast a model and three 3"x6" cylinders. An example of determining mix proportions for a 15 pound batch follows:

Ratio F:S:W:
1:.8:.25

Mix 15 pounds total weight

$$\text{Gypsum} \quad \frac{1}{2.05} (15\#) = 7.317\# = 3319.0 \text{ g}$$

$$\text{Sand (Total)} \quad \frac{.8}{2.05} (15\#) = 5.8536\#$$

$$(\text{Retained on \#50 sieve}) .20(5.8536\#) = 1.1707\# = 531.0 \text{ g}$$

$$(\text{Retained on \#100 sieve}) .70(5.8536\#) = 4.0975\# = 1858.6 \text{ g}$$

$$(\text{Retained on \#200 sieve}) .10(5.8536\#) = .5854\# = 265.5 \text{ g}$$

$$\text{Water} \quad \frac{.25}{2.05} (15\#) = 1.8293\# = 829.7 \text{ g}$$

- 5) Place the sand and gypsum in the mixing bowl. Do not add the water at this time. Mix the sand and gypsum until well blended, 2 to 3 minutes.
- 6) With the mixer off, make a conical depression in the sand and gypsum mixture. Poor the water into the depression, allowing it to soak in for one minute.
- 7) Turn the mixer on, mixing until homogeneous (no dry sand and gypsum visible), 1 to 1 1/2 minutes.

- 8) Turn mixer off. The microconcrete is ready for placement. It must be placed within 7 to 10 minutes after mixing, as the set time is rapid.

Notes:

- a. Sieving the sand is a large consumer of time. It is best to process 50 pounds or more at a time, and store it for future use. The sand should be stored in air tight containers prior to use to avoid any increase in water content.
- b. Avoid contact between skin and gypsum. Gypsum's affinity to water will cause water to be drawn out of the skin. Gypsum is however, non-toxic, non-allergenic, and non-dermatitic.

2. Microreinforcement

Materials: 28-, 24-, 22-gauge black-annealed wire (manufactured by Anchor Wire corp., Goodlettsville, Tenn.)

Equipment: Micrometer
Deforming machine
Thickness gauge
Loading pail and weights
Wire end connections

Table A-1. Details for each miniaturized reinforcing bar to be used as reference in the following procedure.

Bar No.	Dia. (in.)	Knurl (teeth per in.)	Knurl Spacing (in.)	Preload (lb.)
28	.0162	80	.014	9.3
24	.0230	80	.020	18.7
22	.0286	50	.025	28.9

Procedure:

- 1) Place knurls in the deforming machine and set the spacing using the thickness gauge (refer to Table A-1).
- 2) Using the micrometer, check the diameter of the wire in several places to insure that the dimension is as specified in Table A-1 ($\pm 3\%$).
- 3) Deform a length of wire by pulling it through the deforming machine.
- 4) Attach the end connections shown in Figure 12. Hang the wire by one end and attach the loading pail to the other end. Add weights until the preload specified in Table A-1 is reached.

- 5) Remove the weights, loading pail, and lower end connection. The miniaturized reinforcement is prepared.

Notes:

- a. A vice grip attached to the pulling end of the wire helps in the deforming process. Guide the wire by hand into the back of the deformer.
- b. Deform and preload the longest length of wire possible. This length is usually determined by the maximum height above the floor from which the wire may be hung. After removal of the load and lower end connection, leave the wire hanging to prevent kinking caused by handling in the period prior to placing. Cut off lengths of the hanging wire as it (the miniaturized reinforcement) is ready to be placed in the model formwork.

3. Formwork

Material: Plexiglass

Plexiglass is an ideal material for the construction of model formwork. Its main advantages include:

- 1) Availability. Plexiglass is commercially available in a wide range of thicknesses. It is manufactured to a high degree of thickness invariability and has asperity free surfaces.
- 2) Material transparency. Simplifies placing of the miniaturized reinforcement and allows observation of the microconcrete as it is poured into the forms.
- 3) Machineability. Plexiglass is very easy to machine, and low tolerances are easily obtained. The material responds well to cutting, drilling, gluing, and tapping for screw connections.
- 4) Durability. During the reinforced beam test, 13 beams were cast in one plexiglass form with no degradation of dimensional accuracy.
- 5) Inadherency to microconcrete. The extreme smoothness of the plexiglass allows the microconcrete to be cast in and removed from a "dry" form, without the need of a lubricant. A lubricant, which occupies volume, could be detrimental to the dimensional accuracy required for modelling at the small scales required for the GLCM project.

The miniaturized reinforcement is supported at its ends by the formwork. This is accomplished by fitting it through small holes in the

formwork and attaching a crimp to the free ends exposed outside of the forms. An individual hole is drilled for each support and is located relative to the desired placement position of the miniaturized reinforcement. The total number of holes required is equal to two times the number of miniaturized reinforcing bars. The crimps are those sold for tying off wire fishing leaders, and are basically metal sleeves which are mashed to the wire with pliers.

B. MODEL CONSTRUCTION

Components: Microconcrete
Miniaturized reinforcement
Formwork

Additional Materials: Acetone
Crimps
Shellac

Equipment: Needlenose pliers
Mason's trowel
Vibrating table
Paintbrush, 1 inch wide

Procedure:

- 1) CLEAN UNASSEMBLED FORMWORK. Remove any foreign substance from formwork before assembling. Wash in soapy water with soft cloth or sponge. Do not scrape or use wire brush, as plexiglass scratches easily.
- 2) ASSEMBLE FORMWORK. Check inside dimensions and correct for error by adjusting screw tightnesses.
- 3) PLACE MINIATURIZED REINFORCEMENT IN FORMS.
 - a. Cut the deformed and preloaded miniaturized reinforcement to bar lengths equal to the length of span plus 2 inches. The additional 2 inches accounts for form thickness and overhang on which the crimps are to be fastened.
 - b. Slide the microreinforcing bar through the holes in the formwork at both ends, spanning the length of the form. This is difficult to do by hand because of the limited amount of working space. Use needlenose pliers, or even a tweezer or surgical clamp if necessary, to grip and guide the bar.

- c. Using a pair of needlenose pliers, mash a crimp to both ends of the bar which are extending outside the formwork. The crimp must be snug against the outside of the formwork in order to hold the bar in place. Care must be taken not to place the reinforcement in tension.
- d. Repeat steps b and c until all bars are placed.

- 4) PLACE MICROCONCRETE. Place the prepared microconcrete in the form. The consistency of the microconcrete is stiff after mixing. It should be pushed down into the forms and then vibrated. When vibrated, the microconcrete liquifies and flows nicely. Discontinue vibrating when the forms are full and the air is removed. Smooth the top of the microconcrete with the trowel, screeding off excess.

Microconcrete cylinders for compression testing should be cast in conjunction with the casting of each model. Follow the procedures outlined below for the preparation of test cylinders.

- 5) REMOVE FORMWORK. The formwork should be removed 1 to 3 hours after casting. The initial curing process releases heat. Do not remove the formwork until the majority of the heat dissipates.

The crimps must be removed before the forms may be disassembled. The best way to accomplish this is to use the pliers to mash them back to approximately their original shape at which they may be slipped off the ends of the bars. Cutting off the excess bar simplifies the disassembling process.

- 6) CURE AND SEAL MODEL. Allow the model to cure at room temperature for 48 hours.

After 48 hours have elapsed, coat the model with two applications of shellac. The second application should follow the first by 15 minutes.

Sealing the model in this manner prevents further curing and holds the model properties constant for a minimum of 4 days.

C. PREPARATION OF TEST CYLINDERS

Materials: 3" diameter by 5" long cylindrical concrete molds
Microconcrete
Sulfur capping compound

Equipment: 1/2" diameter by 1' long tamp
Vibrating table

Procedure:

- 1) A test cylinder should be cast using three equal layers, 25 tamps per layer, and vibration of 15 seconds duration per layer. The last layer should be screeded flush with the top of the cylinder.
- 2) Remove the cylinder from the mold 2 to 4 hours after casting.

- 3) Allow the cylinder to cure at room temperature for 48 hours.
- 4) Coat the cylinder with two applications of shellac. The second application should follow the first by 15 minutes. Sealing the test cylinder prevents further curing and holds the properties constant for a minimum of 4 days.
- 5) Cylinders to be used in compression testing should be capped using a sulfur capping compound.

END

FILMED

6-86

DTIC